NASA TECHNICAL NOTE

NASA TN D-7286

NASA TN D-7286

A FINITE ELEMENT FOR THERMAL STRESS ANALYSIS OF SHELLS OF REVOLUTION

by Howard M. Adelman, Harold C. Lester, and James L. Rogers, Jr.

Langley Research Center
Hampton, Va. 23665

NATIONAL AERONAUTICS AND SPACE ADMINISTRATION • WASHINGTON, D. C. • DECEMBER 1973

1. Report No.	2. Government Accession No.	3. Recipient's Catalog No.
NASA TN D-7286		

4. Title and Subtitle	5. Report Date
A FINITE ELEMENT FOR THERMAL STRESS ANALYSIS OF SHELLS OF REVOLUTION	December 1973
	6. Performing Organization Code

7. Author(s)	8. Performing Organization Report No.
Howard M. Adelman, Harold C. Lester, and James L. Rogers, Jr.	L-8679
	10. Work Unit No. 501-22-01-01
9. Performing Organization Name and Address	11. Contract or Grant No.
NASA Langley Research Center Hampton, Va. 23665	
	13. Type of Report and Period Covered
12. Sponsoring Agency Name and Address	Technical Note
National Aeronautics and Space Administration Washington, D.C. 20546	14. Sponsoring Agency Code

15. Supplementary Notes

16. Abstract

This report describes a new finite element for performing detailed thermal stress analysis of thin orthotropic shells of revolution. The element provides for temperature loadings which may vary over the surface of the shell as well as through the thickness. In a number of sample calculations, results from the present method are compared with analytical solutions as well as with independent numerical analyses. Such calculations are carried out for two cylinders, a conical frustum, a truncated hemisphere, and an annular plate. Generally, the agreement between the present solution and the other solutions is excellent.

17. Key Words (Suggested by Author(s))	18. Distribution Statement
Shell of revolution Finite-element method Thermal stress	Unclassified – Unlimited

19. Security Classif. (of this report)	20. Security Classif. (of this page)	21. No. of Pages	22. Price*
Unclassified	Unclassified	57	Domestic, $3.50 Foreign, $6.00

*For sale by the National Technical Information Service, Springfield, Virginia 22151

A FINITE ELEMENT FOR THERMAL STRESS ANALYSIS OF SHELLS OF REVOLUTION

By Howard M. Adelman, Harold C. Lester, and James L. Rogers, Jr.
Langley Research Center

SUMMARY

This report describes a new axisymmetric finite element for calculating static thermal stresses in general orthotropic thin shells of revolution. The element is geometrically exact and the thermal loading conditions allow for variations over the shell surface as well as through the shell thickness.

The element is utilized in a number of sample calculations on a variety of shell shapes and loading conditions. Among the shells analyzed are two cylinders, a conical frustum, a truncated hemisphere, and an annular plate. Results from the present method are compared with either exact solutions which are developed in the report or with results from other methods based on finite differences. The results predicted by the present method were found to be in excellent agreement with the exact solutions and the finite-difference solutions.

INTRODUCTION

The capability to predict reliably the static stress of structural components subjected to thermal loads has become an urgent need for structural designers and analysts. Of particular interest are aerospace vehicles undergoing aerodynamic heating during atmospheric entry and aircraft structures heated by impinging jet engine exhaust. In many instances the aerospace vehicles of interest are thin shells of revolution. Closed-form analytical solutions to thermal stress problems for this class of structure have been obtained only for limited geometries and loading conditions (refs. 1 to 3). For more general geometries and loadings it is usually necessary to resort to approximate methods such as finite differences (refs. 4 to 6), numerical integration (ref. 7), or the finite-element method (ref. 8). Finite-difference methods and numerical integration techniques have been used with a good deal of success for thermal stress analysis of shells of revolution with a high degree of generality in the thermal loadings.

The finite-element method has developed into the primary analysis tool for complex structures such as complete aerospace vehicles. Large comprehensive finite-element programs such as NASTRAN (ref. 8) have a variety of finite elements available to the user for modeling almost any conceivable configuration. However the elements themselves, especially the shell of revolution elements, are quite primitive both with regard to their shape and the generality of thermal loads that can be applied, particularly when compared

with the generality available in the previously mentioned approaches. It appears then that the finite-element method can be made more useful with regard to thermal stress analysis by introducing new and/or improved elements which have the kind of generality that is available in the finite-difference and numerical integration approaches. Accordingly, an improved axisymmetric finite element for thermal stress analysis of shells of revolution has been developed.

The purpose of the present report is to describe and evaluate the new finite element. The finite element is geometrically exact, a concept previously utilized for analysis of free vibrations (refs. 9 and 10) and of temperature distributions in shells of revolution (ref. 11).

The report contains a description of the mathematical development of governing matrices for the element and describes a number of sample calculations carried out to verify the accuracy and versatility of the element. These calculations are performed for cylinders under two different loading conditions, a conical frustum, a truncated hemisphere, and an annular plate. Wherever possible analytical solutions (some derived herein) are used for checking results. There are three appendixes to this report. Appendix A contains a summary of the basic equations governing the finite element; appendix B contains the derivation of the thermal stress in an annular plate under a quadratically varying temperature; and appendix C contains a method for obtaining exact modal solutions for thermal stresses in freely supported cylinders.

SYMBOLS

a — inner radius of annular plate (appendix B)

$a_{0,k}, a_{1,k}, a_{2,k}, a_{3,k}, a_{4,k}, a_{5,k}$ — coefficients in polynomial displacement function for normal displacement w

b — outer radius of annular plate (appendix B)

$b_{0,k}, b_{1,k}, b_{2,k}, b_{3,k}$ — coefficients in polynomial displacement function for meridional displacement u

$$C_n = \begin{cases} 2\pi & (n = 0) \\ \pi & (n \neq 0) \end{cases}$$

C_{11}, C_{12}, C_{22} — membrane stiffnesses

C_{66} — in-plane shear stiffness

$c_{0,k}$, $c_{1,k}$, $c_{2,k}$, $c_{3,k}$	coefficients in polynomial displacement function for circumferential displacement v
D_{11}, D_{12}, D_{22}	flexural stiffnesses
D_{66}	torsional stiffness
E_1, E_2	Young's modulus for meridional and circumferential directions, respectively
e_1, e_2	middle-surface strains in meridional and circumferential directions, respectively
e_{12}	middle-surface shear strain
e_1^t, e_2^t, e_{12}^t	total strains
$\{F\}$	thermal force column matrix for complete shell
$\{F_k\}$	element thermal force column matrix
$\{f\}$	thermal force column matrix (see eqs. (12) and (13))
$\{\bar{f}\}$	modal force column matrix (eq. (29))
G	shear modulus
h	shell thickness
$[I]$	identity matrix
$i = \sqrt{-1}$	
K	number of finite elements used to represent shell
K_{11}, K_{12}, K_{22}, K_{66}	stiffnesses representing interaction between in-plane and out-of-plane strains

L	meridional length of shell
M_{t1}, M_{t2}	thermal moment resultants in meridional and circumferential directions, respectively
M_1, M_2, M_{12}	moment resultants in meridional and circumferential directions and twisting moment, respectively
m	meridional wave number for freely supported cylinder
N	order of stiffness matrix and force vector after edge constraints have been applied
N_{t1}, N_{t2}	thermal forces in meridional and circumferential directions, respectively
n	circumferential wave number
R_1, R_2	principal radii of curvature of shell
r	radius of shell measured in plane normal to shell axis
$[S]$	shell stiffness matrix
s	meridional coordinate
T	temperature
T_i, T_o	temperatures at inner and outer fiber of shell, respectively
$[T_k]$	matrix relating coefficients of assumed displacement shapes to degrees of freedom on edges of element
T_{max}	maximum value of temperature
T_1, T_2	stress resultants in meridional and circumferential directions, respectively

T_{12}	shear stress resultant
U	total potential energy
u	meridional component of middle-surface displacement
V	strain energy
v	circumferential component of middle-surface displacement
w	normal component of middle-surface displacement
[X]	matrix which describes assumed form of variables appearing in strain energy
x	meridional coordinate measured within single element
{y}	column matrix containing unknown displacements, rotations, and derivatives thereof
z	coordinate in direction normal to shell surface
α_1, α_2	coefficients of linear thermal expansion in meridional and circumferential directions, respectively
β	rotation of shell generator, $w' - \frac{u}{R_1}$
ϵ_k	length of kth finite element
θ	circumferential coordinate
κ_1, κ_2	changes in curvature in meridional and circumferential directions, respectively
κ_{12}	twist of middle surface
[Λ]	diagonal matrix of eigenvalues of stiffness matrix

λ	eigenvalue of stiffness matrix
λ_m	mode parameter for freely supported cylinder, $m\pi/L$ (appendix C)
μ_1, μ_2	Poisson's ratio for meridional and circumferential directions, respectively
$\{\xi_k\}$	column matrix whose elements are displacements and rotations and their derivatives at ends of kth element
ρ	mass density
σ_1, σ_2	meridional and circumferential stresses, respectively
σ_{12}	shear stress
$[\phi]$	modal matrix for stiffness matrix
Ω	potential energy associated with thermal loading

Subscripts:

k	number of element or number of first edge of element
k+1	number of second edge of element

Superscript:

n	circumferential harmonic number

Primes denote differentiation with respect to s or x; T denotes transpose of a matrix.

ANALYSIS METHOD

In this section of the report, the governing matrix equations are derived. The procedure follows very closely the development in reference 9. The strain energy for a thin orthotropic shell of revolution is derived in terms of the three components of displacement of the shell middle surface and in terms of the shell temperature. A finite-

element representation of the shell is introduced in which the shell is represented by congruent slices of the shell and the displacement components are approximated by polynomials. The potential energy is minimized to obtain the governing matrix equations which involve two main contributions: the stiffness matrix and the thermal load vector. The stiffness matrix is identical to that presented in reference 10. The present development derives the thermal load vector.

Derivation of Governing Equations

Pertinent geometrical quantities are defined in figure 1. The components of displacement in the meridional, circumferential, and normal directions are denoted by u, v, and w, respectively. A point in the shell is defined by the meridional, circumferential, and normal coordinates s, θ, and z, respectively. The two principal radii of curvature of the shell middle surface are R_1 and R_2 and the distance from the axis of the shell to a point on the middle surface is r.

The stress-strain relations for a linear orthotropic material including effects of temperature as given in reference 12 are

$$\left.\begin{aligned}
\sigma_1 &= \frac{E_1}{1 - \mu_1\mu_2}(e_1^t + \mu_2 e_2^t) - \frac{E_1 T}{1 - \mu_1\mu_2}(\alpha_1 + \mu_2\alpha_2) \\
\sigma_2 &= \frac{E_2}{1 - \mu_1\mu_2}(e_2^t + \mu_1 e_1^t) - \frac{E_2 T}{1 - \mu_1\mu_2}(\alpha_2 + \mu_1\alpha_1) \\
\sigma_{12} &= G e_{12}^t
\end{aligned}\right\} \tag{1}$$

where the subscripts 1 and 2 refer to the meridional and circumferential directions, respectively, and $\mu_1 E_2 = \mu_2 E_1$.

The strain energy of the shell modified for a two-dimensional orthotropic material is conveniently written according to reference 13 as

$$U = \frac{1}{2}\int_S\int_\theta\int_Z \left[\sigma_1 e_1^t + \sigma_2 e_2^t + \sigma_{12} e_{12}^t - (\alpha_1\sigma_1 + \alpha_2\sigma_2)T\right] r\, dz\, d\theta\, ds \tag{2}$$

It is assumed that lines originally normal to the middle surface remain straight, unextended, and normal after deformation. The total strains then have the following variation through the shell thickness:

$$\left.\begin{aligned} e_1^t(s,\theta,z) &= e_1(s,\theta) + z\kappa_1(s,\theta) \\ e_2^t(s,\theta,z) &= e_2(s,\theta) + z\kappa_2(s,\theta) \\ e_{12}^t(s,\theta,z) &= e_{12}(s,\theta) + 2z\kappa_{12}(s,\theta) \end{aligned}\right\} \tag{3}$$

Substituting equations (3) into equation (2), rearranging, and discarding a constant involving the known temperature yield:

$$U = V - \Omega \tag{4}$$

where

$$\begin{aligned} V = {} & \frac{1}{2}\iint (C_{11}e_1^2 + 2C_{12}e_1e_2 + C_{22}e_2^2 + C_{66}e_{12}^2)r\ d\theta\ ds \\ & + \frac{1}{2}\iint (D_{11}\kappa_1^2 + 2D_{12}\kappa_1\kappa_2 + D_{22}\kappa_2^2 + D_{66}\kappa_{12}^2)r\ d\theta\ ds \\ & + \frac{1}{2}\iint (K_{11}e_1\kappa_1 + K_{12}(\kappa_1e_2 + \kappa_2e_1) + K_{22}e_2\kappa_2 + K_{66}e_{12}\kappa_{12})r\ d\theta\ ds \end{aligned} \tag{5}$$

$$\Omega = \iint (N_{t1}e_1 + M_{t1}\kappa_1 + N_{t2}e_2 + M_{t2}\kappa_2)r\ d\theta\ ds \tag{6}$$

In equation (5), V is the strain energy of the shell which is utilized in the development of the stiffness matrix in references 9 and 10 and presented in this report for completeness. The stiffnesses in equation (5) are needed in a later section of the report and are given in table 1. The rest of the present development consists of operating on the thermal potential energy Ω to obtain the thermal load vector.

In equation (6), the quantities N_{t1} and N_{t2} are thermal forces and M_{t1} and M_{t2} are thermal moments which are defined as follows:

$$N_{t1} = \int_z \frac{E_1(\alpha_1 + \mu_2\alpha_2)}{1 - \mu_1\mu_2}\, T(s,\theta,z)\, dz \tag{7a}$$

$$N_{t2} = \int_z \frac{E_2(\alpha_2 + \mu_1 \alpha_1)}{1 - \mu_1 \mu_2} T(s,\theta.z)\, dz \tag{7b}$$

$$M_{t1} = \int_z \frac{E_1(\alpha_1 + \mu_2 \alpha_2)}{1 - \mu_1 \mu_2} T(s,\theta,z)\, z\, dz \tag{7c}$$

$$M_{t2} = \int_z \frac{E_2(\alpha_2 + \mu_1 \alpha_1)}{1 - \mu_1 \mu_2} T(s,\theta,z)\, z\, dz \tag{7d}$$

The components of displacement and the temperature are assumed to have the following separable forms for each harmonic n:

$$\left.\begin{aligned} u(s,\theta) &= u(s) \cos n\theta \\ v(s,\theta) &= v(s) \sin n\theta \\ w(s,\theta) &= w(s) \cos n\theta \\ T(s,\theta,z) &= T(s,z) \cos n\theta \end{aligned}\right\} \tag{8}$$

The strain displacement relations used are those of Novozhilov as used in reference 9 and repeated here for completeness:

Middle-surface strains:

$$\left.\begin{aligned} e_1 &= u' + \frac{w}{R_1} \\ e_2 &= \frac{1}{r}\frac{\partial v}{\partial \theta} + \frac{r'}{r} u + \frac{w}{R_2} \\ e_{12} &= \frac{1}{r}\frac{\partial u}{\partial \theta} + v' - \frac{r'}{r} v \end{aligned}\right\} \tag{9}$$

Changes of curvature:

$$\left.\begin{aligned}
\kappa_1 &= -w'' + \frac{1}{R_1}\dot{u}' - \frac{R_1'}{R_1^2}u \\
\kappa_2 &= -\frac{1}{r^2}\frac{\partial^2 w}{\partial\theta^2} + \frac{1}{rR_2^2}\frac{\partial v}{\partial\theta} - \frac{r'}{r}w' + \frac{r'}{rR_1}u \\
\kappa_{12} &= -\frac{1}{r}\frac{\partial w'}{\partial\theta} + \frac{r'}{r^2}\frac{\partial w}{\partial\theta} + \frac{1}{rR_1}\frac{\partial u}{\partial\theta} + \frac{1}{R_2}v' - \frac{r'}{rR_2}v
\end{aligned}\right\} \qquad (10)$$

The thermal forces and moments as well as the strains and changes of curvature are written in separated forms consistent with equations (8)

$$\left.\begin{aligned}
N_{t1} &= N_{t1}\cos n\theta \\
N_{t2} &= N_{t2}\cos n\theta \\
M_{t1} &= M_{t1}\cos n\theta \\
M_{t2} &= M_{t2}\cos n\theta \\
e_1 &= e_1\cos n\theta \\
e_2 &= e_2\cos n\theta \\
e_{12} &= e_{12}\sin n\theta \\
\kappa_1 &= \kappa_1\cos n\theta \\
\kappa_2 &= \kappa_2\cos n\theta \\
\kappa_{12} &= \kappa_{12}\sin n\theta
\end{aligned}\right\} \qquad (11)$$

where N_{t1}, N_{t2}, M_{t1}, and so forth are functions of s only. Substituting equations (9) and (10) along with equations (11) into equation (6) yields

$$\Omega = C_n \int \left\{w, w', w'', u, u', v, v'\right\}^T \{f\}\, ds \tag{12}$$

where $\{f\}$ is a 7×1 column matrix whose elements are given in the following equations:

$$\left.\begin{aligned}
f_1 &= \frac{r}{R_1} N_{t1} + \frac{r}{R_2} N_{t2} + \frac{n^2}{r} M_{t2} \\
f_2 &= -r' M_{t2} \\
f_3 &= -r M_{t1} \\
f_4 &= r' N_{t2} - \frac{r}{R_1^2} R_1' M_{t1} + \frac{r'}{R_1} M_{t2} \\
f_5 &= r N_{t1} + \frac{r}{R_1} M_{t1} \\
f_6 &= r N_{t2} + \frac{r}{R_2} M_{t2} \\
f_7 &= 0
\end{aligned}\right\} \tag{13}$$

The integration with respect to θ from 0 to 2π has been performed and use was made of the following results:

$$C_n = \int_0^{2\pi} \cos^2 n\theta \, d\theta = \begin{cases} 2\pi & (n = 0) \\ \pi & (n > 0) \end{cases}$$

$$S_n = \int_0^{2\pi} \sin^2 n\theta \, d\theta = \begin{cases} 0 & (n = 0) \\ \pi & (n > 0) \end{cases}$$

The thermal forces N_{t1} and N_{t2} as well as the thermal moments M_{t1} and M_{t2} are dependent on the nature of the temperature variation through the shell thickness. (See eqs. (7).) One important case is that of a linear variation through the thickness. For later use, the thermal forces and moments will be evaluated for this special case. If the temperature varies linearly from T_i at the inner face ($z = -h/2$) to T_o at the outer face ($z = h/2$), then

$$T(s, z) = \frac{T_o + T_i}{2} + z \frac{T_o - T_i}{h} \tag{14}$$

where T_o and T_i are functions of s. Substituting equation (14) into equations (7) and integrating through the shell thickness give

$$\left.\begin{aligned}
N_{t1} &= (\alpha_1 C_{11} + \alpha_2 C_{12}) \frac{T_o + T_i}{2} + (K_{11}\alpha_1 + K_{12}\alpha_2) \frac{T_o - T_i}{h} \\
N_{t2} &= (\alpha_1 C_{12} + \alpha_2 C_{22}) \frac{T_o + T_i}{2} + (K_{12}\alpha_1 + K_{22}\alpha_2) \frac{T_o - T_i}{h} \\
M_{t1} &= (\alpha_1 D_{11} + \alpha_2 D_{12}) \frac{T_o - T_i}{h} + (K_{11}\alpha_1 + K_{12}\alpha_2) \frac{T_o + T_i}{2} \\
M_{t2} &= (\alpha_1 D_{12} + \alpha_2 D_{22}) \frac{T_o - T_i}{h} + (K_{12}\alpha_1 + K_{22}\alpha_2) \frac{T_o + T_i}{2}
\end{aligned}\right\} \tag{15}$$

These forms for the thermal forces and moments complete the development of the column matrix $\{f\}$ in equations (13) for the special case of a linear temperature distribution through the shell thickness.

The next step in the development is to write Ω for a single finite element in order to be able to arrive at the required thermal load vector for an element. The basis for these operations is described in references 9 and 10; for completeness, the essential concepts are summarized in appendix A. Combining equations (A2), (A5), and (12) yields the following form of the thermal potential energy for the kth element:

$$\Omega_k = \left\{\xi_k\right\}^T \left\{F_k\right\} \tag{16}$$

where $\{F_k\}$ is the thermal load column matrix for the kth element as given by

$$\{F_k\} = C_n [T_k]^T \int_{-\epsilon_k/2}^{\epsilon_k/2} [X]^T \{f\} \, dx \tag{17}$$

Formulation and Solution of Final Equations

As in reference 10, the following conditions of compatibility are imposed at each element juncture:

$$\begin{Bmatrix} w_{k+1} \\ u_{k+1} \\ v_{k+1} \\ \beta_{k+1} \\ u'_{k+1} \\ v'_{k+1} \\ \beta'_{k+1} \end{Bmatrix}_{k \text{ element}} = \begin{Bmatrix} w_{k+1} \\ u_{k+1} \\ v_{k+1} \\ \beta_{k+1} \\ u'_{k+1} \\ v'_{k+1} \\ \beta'_{k+1} \end{Bmatrix}_{k+1 \text{ element}} \qquad (k < K) \tag{18}$$

Of the seven conditions of compatibility shown in equation (18), only the first four are strictly required to assure that the element converges. The last three conditions are imposed in order to improve the convergence characteristics of the element. Specifically, these conditions require continuity of strains and change of curvature at element junctures and evidence of the improved accuracy resulting from this continuity has been presented in reference 12.

Two final observations are that the last three conditions are not correct for shells which have a step discontinuity in stiffness at an element juncture and that for problems in which the theoretical stress distribution has a slope discontinuity, the present element will display a "rounded corner" at the location of the slope discontinuity.

The total thermal potential energy is obtained by summing the element contributions; thus,

$$\Omega = \sum_{k=1}^{K} \Omega_k \tag{19}$$

where Ω_k is given in equation (16). When the summation indicated in equation (19) is carried out and use is made of equations (17) and (18), the thermal potential energy may be written as

$$\Omega = \{y\}^T \{F\} \tag{20}$$

where

$\{F\}$ thermal load column matrix of order $7(K + 1)$

$\{y\}$ column matrix containing the unknown displacements, rotations, and derivatives thereof

From reference 9, the strain energy may be written

$$V = \frac{1}{2} \{y\}^T [S] \{y\} \tag{21}$$

where $[S]$ represents the stiffness matrix which is a symmetric positive definite or positive semidefinite matrix of order $7(K + 1)$. The formation of the stiffness matrix has been described in references 9 and 10 and need not be discussed further. The formation of the thermal force column matrix for the complete shell from the element thermal force column matrices is accomplished by overlapping the last seven numbers in each column matrix with the first seven numbers in the adjacent (higher numbered) column matrix. Finally the column matrix $\{y\}$ is the union of the column matrices $\{\xi_k\}$ as defined in equation (A6).

The equations governing the behavior of the shell before edge constraints are applied are derived by minimizing the total potential energy. Thus,

$$\delta(V - \Omega) = 0 \tag{22}$$

The minimization in equation (22) is equivalent to the following matrix equation:

$$[S]\{y\} = \{F\} \tag{23}$$

Edge constraints are incorporated by deleting appropriate rows and columns from $[S]$ and rows from $\{F\}$. In table 2, the rows and columns deleted for various edge conditions are given. It is noted that the degrees of freedom of the edges constitute the first seven rows of $\{y\}$ and the last seven rows of $\{y\}$. Further, it is only the first four of these in each group namely w, u, v, and β that are involved in the definition of edge constraints. Accordingly, as shown in table 2 the only rows and columns that are ever deleted from the $[S]$ matrix and the $\{F\}$ matrix are among the first four and $7K + 1$, $7K + 2$, $7K + 3$, and $7K + 4$ rows and columns.

The stiffness matrix is nonsingular if and only if the edge constraints are sufficient to prevent all possible rigid body motions of the shell. In this case, equation (23) may be solved by any of a number of standard methods for solving sets of simultaneous linear equations. Unfortunately in practical shell problems there are situations wherein the edge conditions are not sufficient to prevent all rigid body motion and the standard methods are not applicable. For example a free-free shell under a self-equilibrating set of loads has a singular stiffness matrix and more importantly (for this paper) so does a shell with an insufficient set of edge constraints under any applied thermal loading. Equation (23) cannot be solved for either of these classes of problems without a solution technique which is not dependent on the nonsingularity of the stiffness matrix. For this reason the solution of equation (23) is carried out by a method normally used for dynamics problems – that is, an eigenvector expansion. Let

$$\{y\} = [\phi]\{q\} \tag{24}$$

where $[\phi]$ is the matrix of eigenvectors of the stiffness matrix in which each column is an eigenvector denoted by $\{\phi\}$ and $\{q\}$ is the column matrix of modal coordinates. Thus, $\{\phi\}$ and λ satisfy the equation

$$[S]\{\phi\} = \lambda\{\phi\} \tag{25}$$

The eigenvectors are normalized so that

$$[\phi]^T[\phi] = [I] \tag{26}$$

Then

$$[\phi]^T[S][\phi] = [\Lambda] \tag{27}$$

where

$$[\Lambda] = \begin{bmatrix} \lambda_1 & & & & \\ & \lambda_2 & & & \\ & & \cdot & & \\ & & & \cdot & \\ & & & & \cdot \\ & & & & \lambda_N \end{bmatrix} \tag{28}$$

Substituting equation (24) into equation (23), premultiplying by $[\phi]^T$, and making use of equation (27) give

$$[\Lambda]\{q\} = \{\bar{f}\} \tag{29}$$

where $\{\bar{f}\} = [\phi]^T\{F\}$ is the generalized force column matrix in which the ith element of $\{\bar{f}\}$ is the component of force that would deform the shell into the shape characterized by the ith eigenvector of $[S]$. The solution of equation (29) is as follows

$$q_i = \begin{cases} \bar{f}_i/\lambda_i & (\lambda_i \neq 0) \\ 0 & (\lambda_i = 0) \end{cases} \qquad (i = 1, 2, \ldots, N) \tag{30}$$

The column matrix $\{y\}$ is then obtained from equation (24).

Displacement and Stress Recovery

The coefficients of the polynomials representing the displacement field are obtained from equation (A5). The displacement components u, v, and w are then obtained by use of the equations:

$$\left.\begin{aligned} w &= a_{0,k} + a_{1,k}x + a_{2,k}x^2 + a_{3,k}x^3 + a_{4,k}x^4 + a_{5,k}x^5 \\ u &= b_{0,k} + b_{1,k}x + b_{2,k}x^2 + b_{3,k}x^3 \\ v &= c_{0,k} + c_{1,k}x + c_{2,k}x^2 + c_{3,k}x^3 \end{aligned}\right\} \tag{31}$$

The middle-surface strains and changes of curvature are obtained from equations (9) and (10). The fiber strains are obtained from equations (3) by substituting $\pm h/2$ for z and are as follows:

$$\left.\begin{aligned} e_1^t\left(s,\theta,\pm\frac{h}{2}\right) &= e_1(s,\theta) \pm \frac{h}{2}\,\kappa_1(s,\theta) \\ e_2^t\left(s,\theta,\pm\frac{h}{2}\right) &= e_2(s,\theta) \pm \frac{h}{2}\,\kappa_2(s,\theta) \\ e_{12}^t\left(s,\theta,\pm\frac{h}{2}\right) &= e_{12}(s,\theta) \pm \frac{h}{2}\,\kappa_{12}(s,\theta) \end{aligned}\right\} \tag{32}$$

The plus (+) sign denotes the outer fiber and the minus (-) sign denotes the inner fiber. The stress resultants T_1, T_2, and T_{12} and the moments resultants M_1, M_2, and M_{12} are defined as follows:

$$\left.\begin{aligned} T_1 &= \int_{-h/2}^{h/2} \sigma_1\,dz & M_1 &= \int_{-h/2}^{h/2} \sigma_1 z\,dz \\ T_2 &= \int_{-h/2}^{h/2} \sigma_2\,dz & M_2 &= \int_{-h/2}^{h/2} \sigma_2 z\,dz \\ T_{12} &= \int_{-h/2}^{h/2} \sigma_{12}\,dz & M_{12} &= \int_{-h/2}^{h/2} \sigma_{12} z\,dz \end{aligned}\right\} \tag{33}$$

Substituting equations (1) along with equations (3) into equations (33) and using the definition in table 1 yields the following expressions:

$$
\left.
\begin{aligned}
T_1 &= C_{11}e_1 + C_{12}e_2 + K_{11}\kappa_1 + K_{12}\kappa_2 - N_{t1} \\
T_2 &= C_{12}e_1 + C_{22}e_2 + K_{12}\kappa_1 + K_{22}\kappa_2 - N_{t2} \\
T_{12} &= C_{66}e_{12} + K_{66}\kappa_{12} \\
M_1 &= D_{11}\kappa_1 + D_{12}\kappa_2 + K_{11}e_1 + K_{12}e_2 - M_{t1} \\
M_2 &= D_{12}\kappa_1 + D_{22}\kappa_2 + K_{12}e_1 + K_{22}e_2 - M_{t2} \\
M_{12} &= \frac{1}{2} D_{66}\kappa_{12} + \frac{1}{2} D_{66}e_{12}
\end{aligned}
\right\} \qquad (34)
$$

The displacements and stress and moment resultants are evaluated for specified values θ_i according to the following formulas:

$$u(\theta_i,s) = \sum_n u(s) \cos n\theta_i \qquad (i = 1, 2, \ldots) \qquad (35a)$$

$$v(\theta_i,s) = \sum_n v(s) \sin n\theta_i \qquad (i = 1, 2, \ldots) \qquad (35b)$$

$$w(\theta_i,s) = \sum_n w(s) \cos n\theta_i \qquad (i = 1, 2, \ldots) \qquad (35c)$$

$$T_1(\theta_i,s) = \sum_n T_1(s) \cos n\theta_i \qquad (i = 1, 2, \ldots) \qquad (35d)$$

$$T_2(\theta_i,s) = \sum_n T_2(s) \cos n\theta_i \qquad (i = 1, 2, \ldots) \qquad (35e)$$

$$T_{12}(\theta_i,s) = \sum_n T_{12}(s) \sin n\theta_i \qquad (i = 1, 2, \ldots) \qquad (35f)$$

$$M_1(\theta_i,s) = \sum_n M_1(s) \cos n\theta_i \qquad (i = 1, 2, \ldots) \qquad (35g)$$

$$M_2(\theta_i,s) = \sum_n M_2(s) \cos n\theta_i \qquad (i = 1, 2, \ldots) \qquad (35h)$$

$$M_{12}(\theta_i,s) = \sum_n M_{12}(s) \sin n\theta_i \qquad (i = 1, 2, \ldots) \qquad (35i)$$

The range of summation on n is over the number of circumferential harmonics considered.

EVALUATION OF THE ELEMENT

In order to verify the validity and versatility of the new element, sample calculations were performed for a variety of shell geometries and thermal loads. Analytical solutions were available for some of the models. In the following sections are presented descriptions of the shells, the methods of evaluating numerical results, the finite-element representations, and detailed evaluations of the results.

Description of Shells Analyzed

The geometry of the shells analyzed are illustrated in figure 2 along with the corresponding temperature loading functions and the shell material properties. For cylinders I and II and the truncated hemisphere, the temperature is constant through the shell thickness. For the conical frustum and the annular plate, the temperature varies through the thickness. For all shells except cylinder II, which has freely supported edges, the edge conditions are clamped-clamped. Also, the temperatures are axisymmetric except for cylinder II. A brief description of each shell is given as follows:

Cylinder I is a cylindrical shell having a temperature distribution with a discontinuous slope at the midlength of the cylinder (s/L = 1/2). This discontinuity occurs when the midlength circumference is maintained at a prescribed temperature. The temperature distribution (derived in refs. 3 and 11) illustrates the behavior of the present finite element for a stress distribution having a slope discontinuity.

Cylinder II is a cylindrical shell with a temperature distribution which is constant along the length of the shell but varies around the circumference. This temperature distribution (derived in refs. 3 and 11) results when a generator of the cylinder is maintained at a constant temperature. This example was chosen to illustrate the application of the

finite element to a nonaxisymmetric temperature distribution and also to illustrate an application where, because of the freely supported edge conditions, the stiffness matrix is singular.

An orthotropic 30° conical frustum has a temperature distribution which varies quadratically along the shell length and linearly through the thickness. This distribution is an approximation to that in the vicinity of the nose of a missile undergoing aerodynamic heating (ref. 14). This example illustrates the use of the present element for orthotropic shells, for a nonconstant shell radius, and for an applied thermal bending moment.

A truncated hemisphere having a temperature distribution (derived in ref. 11) corresponding to a uniform heat flux over the outer surface of the shell was chosen to illustrate a calculation for a shell with a curved generator such that both principal radii of curvature are nonzero.

An annular plate with a temperature varying linearly through the thickness and quadratically from the inner radius to the outer radius illustrates the application of the element when thermal bending moments are applied as the loads and for the limiting case of an annular plate.

Method of Evaluation

The evaluation of the element was accomplished by using a computer program to calculate stress and moment resultants and then by comparing the results with other solutions for the same configurations. Check solutions were obtained from the following sources:

For cylinder I, an analytical solution was available from reference 3

For cylinder II, a converged modal solution was generated based on the procedure described in appendix C, and results were obtained for harmonics $n = 0$ to 4

For the orthotropic conical frustum, check results were available from the finite-difference computer programs of references 5 and 6

For the truncated hemisphere, a solution was available from reference 5

For the annular plate, an analytical solution derived in appendix B was utilized

Detailed comparisons between results with the present method and results from these sources are presented in a later section.

Finite-Element Representation

The number and spacing of elements in the shell representations are given in table 3. These representations were arrived at by the following procedure: first, each shell

was analyzed with a representation of 10 equally spaced elements and results were compared with the appropriate check solution. If satisfactory agreement was obtained (as for cylinder II and the annular plate), no refinement was performed. If the results were not satisfactory, a more refined representation of the shell was made in the vicinity of the edges of the shells where the steepest gradients in the stress distributions are found. The refinements were similar to those done in the modal stress study of reference 12. The final representations used to give the results in the present report are those in table 3.

Evaluation and Discussion

Calculated results from the present finite-element and other analyses are presented in tables 4 to 8 and in figures 3 to 8. In this section, an evaluation of the performance of the element for each set of calculations is presented. Before proceeding to discussions of individual shells, two general observations are made.

(1) For all shells except cylinder II, results are axisymmetric; that is, they correspond to $n = 0$ because of the axisymmetric character of the temperature loads

(2) For all shells except the annular plate, the moment resultants are negligibly small and are not presented

Cylinder I.- Nondimensional meridional and circumferential stress resultants predicted by the present method for cylinder I are presented along with analytical results from reference 3 in table 4. The stress resultant distributions are necessarily symmetric about the midlength of the cylinder as a consequence of the symmetry of the load and the edge conditions. The analytical solution for this example as given in reference 3 shows a constant meridional stress resultant T_1, whereas the present finite-element solution exhibits a slight oscillation about the constant value. The maximum error of 0.6 percent occurs at the midlength of the cylinder. The comparison for the circumferential stress resultants T_2 also shows close agreement, the largest error being 0.4 percent. In figure 3, the stress resultants are plotted with the analytical solution being represented by the solid curves and the present finite-element solution indicated by the circles. It is of particular interest to observe that the analytical solution for T_2 has a cusp – that is, a discontinuity in the slope at the cylinder midlength as a result of the discontinuity in the slope of the temperature distribution at that location. Since the displacement field assumed for the finite element implies continuity in the slope of the stress resultants it might be expected that the element would have difficulty converging in the vicinity of such a cusp. However as indicated in figure 3, no such difficulty was found, and although there is a local rounding of the cusp, this rounding was too negligible to be plotted and had no appreciable effect on the accuracy of the stress resultant.

Cylinder II.- Circumferential stress resultants T_2 for cylinder II for values of n from 0 to 4 are shown in table 5. In this table, the exact solution was obtained by the modal

superposition method described in appendix C. The stress resultants from the present method are quite close to the exact solution for all values of n in the calculations. Further there is only a slight loss of accuracy with increasing values of n. The results are also shown in figure 4 wherein the present results are indicated by the symbols and the exact solution shown by the solid curves. Because the resultants are symmetric about the midlength of the cylinder, results are plotted for only half the shell. It may be observed from figure 4 that the harmonics of circumferential stress resultants decrease in magnitude toward the midlength of the cylinder and the rapidity of the decay appears to increase with n. A final observation from figure 4 is that all of the harmonics pass through zero at about $s/L = 0.125$ for this particular cylinder.

Figure 5 illustrates the results of performing the Fourier summation of the harmonics by using equations (35) at values of θ of 0°, 45°, and 90° where the angle is measured from the heated generator. Results in this figure are from the present method only.

The meridional stress resultant T_1 was found to be less than 1 percent of the circumferential resultant for all harmonics. This occurrence may be explained by the fact that the freely supported edge conditions require T_1 to vanish at each edge, and for short cylinders such as that used in the present example, T_1 never develops a significant value. For larger cylinders with freely supported edges, T_1 is not small and this point is discussed further in appendix C.

Orthotropic 30° conical frustum.- The meridional stress resultant T_1 for the orthotropic 30° conical frustum which was computed by the present method and solutions from the methods of references 5 and 6 are presented in table 6. The agreement between the present method and reference 6 is excellent with a maximum difference of less than 1 percent which occurs at the smaller edge of the shell. The difference between the present method and reference 5 is somewhat larger, being about 5 percent at the smaller edge and about 3 percent at the larger edge. The solutions are plotted in figure 6 where it can be seen that all three results are in close agreement except in the immediate vicinity of the edges of the shell.

The circumferential stress resultant was negligibly small away from the edges of the shell and significant values occurred only within 1 percent of the shell length from the small edge and 3 percent of the shell length from the large edge. These edge results are summarized in the following table:

Location	Dimensionless circumferential stress resultant in a conical shell, $T_2/Eh\alpha T_{max}$		
	Present analysis	SADAOS (ref. 6)	SALORS (ref. 5)
Smaller end	-28.17	-29.44	-28.89
Larger end	-12.24	-10.82	-12.27

The results are in fair agreement, with the present solution lower than either reference 5 or 6 at the smaller end but bounded by those results at the larger end. The maximum difference is about 13 percent with respect to the results of reference 6 at the larger end. One interesting and unexpected result in this calculation is that even though there is a temperature gradient through the shell thickness and, consequently, a thermal moment applied, the moment resultants were substantially zero. This result was obtained by all three analyses and cannot be rationalized by the authors.

Truncated hemisphere.- Meridional and circumferential stress resultants for the truncated hemisphere which were computed by the present formulation and those from the method of reference 5 are presented in table 7. The agreement is generally good. The only significant differences between the two results occur in the values of the meridional stress resultant at the edges of the shell. There is a difference of about 5 percent at the larger diameter ($s/L = 0$) and about 10 percent at the smaller diameter ($s/L = 1$). There is good agreement between the two solutions for the circumferential stress resultant with a maximum difference of 2 percent which occurs at the larger edge.

The results are shown graphically in figure 7 where the present solution is represented by the symbols and the results of reference 5 are shown as the solid curves. An interesting and encouraging aspect of the comparison of results for this case is that, for the dominant stress resultant T_2, there was excellent agreement and the significant differences occurred in the smaller stress resultant T_1 at a location where it was substantially zero.

Annular plate.- Meridional and circumferential moment results for the annular plate from the finite-element calculation are presented in table 8 together with the analytical solution derived in appendix B. For the meridional moment resultant comparison, the solutions agree to within 0.3 percent except at $s/L = 0.2$ where the present method is 1.2 percent lower than the analytical solution. For the circumferential moment resultant comparison, the solutions agree to within 1 percent except at $s/L = 0.2$ where the two-place agreement at the inner edge and four-place agreement at the present solution is 4 percent lower than the analytical solution.

CONCLUDING REMARKS

A new finite element for thermal stress analysis of orthotropic thin shells of revolution is described. The element is geometrically exact in that no approximation of the shell generator is required. Further, provision is made for the applied thermal loads to vary over the shell surface and through the shell thickness in any mathematically describable fashion.

Sample calculations are carried out on a variety of shell models and results from the present method are compared either with analytical solutions or with numerical results from independent analyses. Among the shell configurations analyzed are cylinders under two different thermal loading conditions, a conical frustum, a truncated hemisphere, and an annular plate. For these calculations the results from the new finite element generally are in good agreement with the check solutions. The only significant inaccuracies were observed in some stress resultants near the clamped edges of the conical frustum and the hemisphere where the stress gradients were particularly severe and consequently where finite-element analyses usually require significant refinement before convergence is obtained.

The nature of the finite element is such that continuity of strains and curvatures is maintained at all points along the shell. Consequently in a shell where there is theoretically a slope discontinuity or cusp in a stress or moment resultant the results predicted by the present method will show a slight local smoothing of the cusp but this has no adverse effect on the accuracy of the results.

Langley Research Center,
National Aeronautics and Space Administration,
Hampton, Va., June 30, 1973.

APPENDIX A

REPRESENTATION OF A SHELL OF REVOLUTION BY GEOMETRICALLY EXACT FINITE ELEMENTS

The basic assumptions underlying the finite element and a detailed derivation of the stiffness matrix are given in references 9 and 10. The purpose of this appendix is to summarize the concepts, conventions, and equations needed in the development of the thermal load vector for a geometrically exact finite element.

The following notation is used (fig. 9):

K	total number of elements used to represent shell
ϵ_k	meridional length of kth finite element
x	coordinate in kth element, measured from center of element so that

$$-\frac{\epsilon_k}{2} \leqq x \leqq \frac{\epsilon_k}{2} \tag{A1}$$

A subscript notation is established in which a subscript k, when used with a quantity such as u, v, w, β, R_1 or their derivatives, implies that the quantity is evaluated at the first edge of the element $x = -\frac{\epsilon_k}{2}$. Similarly, a subscript $k+1$, when used with such quantities, implies that they are evaluated at the second edge of the element $x = \frac{\epsilon_k}{2}$. In all other uses of the subscript k, for example, for matrices and vectors, it means that the quantity with the subscript is evaluated for the kth element. The displacement components or derivatives thereof within the kth element are approximated by polynomials as follows (ref. 10):

$$\begin{Bmatrix} w \\ w' \\ w'' \\ u \\ u' \\ v \\ v' \end{Bmatrix} = [X] \{\gamma_k\} \tag{A2}$$

where

$$[x] = \begin{bmatrix} 1 & x & x^2 & x^3 & x^4 & x^5 & 0 & 0 & 0 & 0 & 0 & 0 & 0 & 0 \\ 0 & 1 & 2x & 3x^2 & 4x^3 & 5x^4 & 0 & 0 & 0 & 0 & 0 & 0 & 0 & 0 \\ 0 & 0 & 2 & 6x & 12x^2 & 20x^3 & 0 & 0 & 0 & 0 & 0 & 0 & 0 & 0 \\ 0 & 0 & 0 & 0 & 0 & 0 & 1 & x & x^2 & x^3 & 0 & 0 & 0 & 0 \\ 0 & 0 & 0 & 0 & 0 & 0 & 0 & 1 & 2x & 3x^2 & 0 & 0 & 0 & 0 \\ 0 & 0 & 0 & 0 & 0 & 0 & 0 & 0 & 0 & 0 & 1 & x & x^2 & x^3 \\ 0 & 0 & 0 & 0 & 0 & 0 & 0 & 0 & 0 & 0 & 0 & 1 & 2x & 3x^2 \end{bmatrix} \tag{A3}$$

and

$$\{\gamma\}^T = \left\lfloor a_{0,k}, a_{1,k}, a_{2.k}, a_{3,k}, a_{4,k}, a_{5,k}, b_{0,k}, b_{1,k}, b_{2,k}, b_{3,k}, c_{0,k}, c_{1,k}, c_{2,k}, c_{3,k} \right\rfloor \tag{A4}$$

The coefficients of the polynomials are related to the variables at the edges of the element by the following relation:

$$\{\gamma_k\} = [T_k]\{\xi_k\} \tag{A5}$$

where the matrix $[T_k]$ is given in table 9 and

$$\{\xi_k\} = \left\lfloor w_k, u_k, v_k, \beta_k, u'_k, v'_k, \beta'_k, w_{k+1}, u_{k+1}, v_{k+1}, \beta_{k+1}, u'_{k+1}, v'_{k+1}, \beta'_{k+1} \right\rfloor \tag{A6}$$

The reader will notice that two new quantities have been introduced into $\{\xi\}$. These are the meridional rotation β and its derivative β' (which is identical to the change in curvature κ_1). The reason for the introduction of these quantities in place of w' and w'' is that in order to perform the necessary superposition of element matrices and vectors, a set of compatibility conditions at element junctures must be formulated and these conditions are convenient to express and are physically meaningful in terms of β and β' rather than w' and w''. The matter of the form of the compatibility conditions at the element junctures is discussed further in the main body of this paper.

APPENDIX B

ANALYTICAL SOLUTION FOR THERMAL STRESSES IN AN ANNULAR PLATE UNDER PURE BENDING

The governing differential equation for the plate is derived in accordance with the following assumptions:

(1) The plate is isotropic, thus

$$\left.\begin{aligned} \alpha_1 &= \alpha_2 = \alpha \\ E_1 &= E_2 = E \\ \mu_1 &= \mu_2 = \mu \end{aligned}\right\} \tag{B1}$$

(2) The temperature loading is axisymmetric

(3) The in-plane displacement components u and v are neglected

For an annular plate having an inner radius a and an outer radius b, the functions describing the reference surface are

$$\left.\begin{aligned} r &= a + s \\ r' &= 1 \\ \frac{1}{R_1} &= \frac{1}{R_2} = R_1' = 0 \end{aligned}\right\} \tag{B2}$$

The principle of minimum potential energy is used to obtain the governing equation. The statement of the principle is

$$\delta (V - \Omega) = 0 \tag{B3}$$

Based on assumptions (1), (2), and (3) and equations (B2), equation (B3) may be written

$$\delta \int_a^b D \left[(w'')^2 + \frac{2\mu}{r} w' w'' + \left(\frac{w'}{r^2}\right)^2 + \frac{2M_t}{D}\left(\frac{w'}{r} + w''\right)\right] r \, dr = 0 \tag{B4}$$

where

$$D = \frac{Eh^3}{12(1 - \mu^2)}$$

and the prime indicates a derivative with respect to r. Carrying out the variations as indicated in equation (B4) yields the required differential equation

$$w^{IV} + \frac{2}{r} w''' - \frac{w''}{r^2} + \frac{w'}{r^3} = - \frac{M_t' - rM_t''}{Dr} \tag{B5}$$

Letting the right side of equation (B5) be represented by a function $M(r)$ and regrouping the left side yield

$$\frac{1}{r} \frac{d}{dr} \left\{ r \frac{d}{dr} \left[\frac{1}{r} \frac{d}{dr} \left(r \frac{dw}{dr} \right) \right] \right\} = M(r) \tag{B6}$$

A solution to equation (B6) is sought which corresponds to a constant value of M. The general solution to equation (B6) with M equal to a constant is

$$w = A + Br^2 + cr^2 \log r + d \log r + \frac{Mr^4}{64} \tag{B7}$$

The changes in curvature and the moment resultants are then calculated by use of equations (10) and (37), respectively. The boundary conditions are taken to be those of clamped edges

$$\left.\begin{aligned} w(a) = w'(a) = 0 \\ w(b) = w'(b) = 0 \end{aligned}\right\} \tag{B8}$$

Substituting equation (B7) into equations (B8) gives the following equation for determining the constants:

APPENDIX B

$$\begin{bmatrix} 1 & a^2 & a^2 \log a & \log a \\ 0 & 2a & a(1 + 2 \log a) & 1/a \\ 1 & b^2 & b^2 \log b & \log b \\ 0 & 2b & b(1 + 2 \log b) & 1/b \end{bmatrix} \begin{Bmatrix} A \\ B \\ c \\ d \end{Bmatrix} = \begin{Bmatrix} -\frac{Ma^4}{64} \\ -\frac{Ma^3}{16} \\ -\frac{Mb^4}{64} \\ -\frac{Mb^3}{16} \end{Bmatrix} \tag{B9}$$

Return now to the determination of a temperature distribution corresponding to a constant value of M and set

$$\frac{-M_t' - rM_t''}{Dr} = M = \text{Constant}$$

then the differential equation for M_{t1} may be written as

$$\frac{d}{dr}(rM_t') = -MDr \tag{B10}$$

Integrating and discarding the constants of integration give

$$M_t = -\frac{MD}{4}r^2 \tag{B11}$$

Using equation (B11) along with the expression for the thermal moment in terms of temperature (eqs. (15)) gives

$$M_t = \frac{\alpha D}{h}(1 + \mu)(T_o - T_i) = -\frac{MD}{4}r^2 \tag{B12}$$

Thus a temperature distribution corresponding to a constant value of M is one in which the temperature difference between the inner and outer fiber of the plate varies quadratically with r. Letting

$$T_o - T_i = \beta r^2 \tag{B13}$$

results in

$$M = \frac{-4\alpha(1 + \mu)\beta}{h} \tag{B14}$$

and

$$M_t = \frac{\alpha D(1 + \mu)\beta r^2}{h} \tag{B15}$$

APPENDIX C

EXACT MODAL SOLUTIONS FOR THERMAL STRESSES IN FREELY SUPPORTED CYLINDERS

In this appendix the nonaxisymmetric state of thermal stress in a freely supported cylindrical shell is determined by a superposition of the free vibration modes. The potential energy for the shell is expressed in terms of middle-surface displacements and the temperature distribution in the shell. The temperature is assumed to be constant through the thickness. The displacement components and temperature distribution are represented in terms of their circumferential Fourier harmonics and each harmonic of stress is determined independently of the others in terms of the same harmonic of temperature.

Symbols

Symbols not previously defined in the main text and/or those unique to this appendix are defined as follows:

k	summation index, $k = 1, 2, 3$ (see eqs. (C4))
$[\bar{K}]$	stiffness matrix, 3×3
$\bar{K}_{11}, \bar{K}_{12}, \bar{K}_{13}, \bar{K}_{22}, \bar{K}_{23}, \bar{K}_{33}$	stiffness coefficients (see eqs. (C7))
m	number of meridional half-waves
$[\bar{M}]$	mass matrix
P_{nm}	generalized force
q_{nmk}	generalized coordinates (see eqs. (C4))
$S_n = \begin{cases} 0 & (n = 0) \\ \pi & (n \neq 0) \end{cases}$	
t	time
T^*	kinetic energy

APPENDIX C

α_{nmk}, β_{nmk}, γ_{nmk}	modal amplitudes (see eqs. (C4))
$\{\bar{\alpha}\}$	column matrix of modal amplitudes
ω_{nmk}	natural frequency of nmk vibration mode

Subscript:

n	nth circumferential harmonic

General Method

The strain-displacement relations used in this appendix are those of Kraus (ref. 15, p. 32) and differ from those in the main text (eqs. (10)) only in the κ_{12} term. The expressions used are

$$\left.\begin{aligned} e_1^t &= u' - zw'' \\ e_2^t &= \frac{1}{r}\frac{\partial v}{\partial \theta} + \frac{w}{r} + z\left(\frac{1}{r^2}\frac{\partial v}{\partial \theta} - \frac{1}{r^2}\frac{\partial^2 w}{\partial \theta^2}\right) \\ e_{12}^t &= \frac{1}{r}\frac{\partial u}{\partial \theta} + v' - z\left(\frac{2}{r}\frac{\partial w'}{\partial \theta} - \frac{1}{r}v'\right) \end{aligned}\right\} \tag{C1}$$

The strain energy U is derived in a manner analogous to that of the main text and is given by

$$U = \sum_{n=0} U_n \tag{C2}$$

where U_n is the contribution to the strain energy due to the nth circumferential harmonic of displacement and temperature and is given by the following equation:

APPENDIX C

$$U_n = \frac{C_n}{2}\int_0^L C\left[u_n'^2 + \frac{n^2}{r^2}v_n^2 + \frac{w_n^2}{r^2} + \frac{2n}{r^2}v_n w_n\right.$$

$$+ \frac{2\mu n}{r}u_n' v_n + \frac{2\mu}{r}u_n' w_n + \left(\frac{1-\mu}{2}\right)\frac{n^2}{r^2}u_n^2$$

$$\left. + S_n\left(\frac{1-\mu}{2}\right)v_n'^2 - \left(\frac{1-\mu}{r}\right)nu_n v_n'\right] r\,ds$$

$$+ C_n\int_0^L D\left[w_n''^2 + \frac{n^2}{r^4}v_n^2 + \frac{n^4}{r^4}w_n^2 + \frac{2n^3}{r^4}v_n w_n\right.$$

$$\left. - \frac{2\mu}{r}w_n''\left(\frac{n}{r}v_n + \frac{n^2}{r}w_n\right) + \left(\frac{1-\mu}{2}\right)\left(\frac{4n^2}{r^2}w_n'^2 + \frac{S_n}{r^2}v_n'^2 + \frac{4n}{r^2}w_n' v_n'\right)\right] r\,ds$$

$$- C_n\int_0^L C(1+\mu)\alpha T\left[u_n' + \frac{n}{r}v_n + \frac{w_n}{r}\right] r\,ds \qquad \text{(C3)}$$

where

$$S_n = \begin{cases} 0 & (n = 0) \\ \pi & (n \neq 0) \end{cases}$$

In equation (C3) the first integral represents the membrane strain energy, the second integral represents the flexural strain energy, and the third integral represents the thermal strain energy.

The displacement components $u_n(s)$, $v_n(s)$, and $w_n(s)$ are expanded in terms of the free vibration modes of a cylinder with freely supported edges (ref. 9). This expansion is as follows:

$$u_n(s) = \sum_{m=1}^{M}\sum_{k=1}^{3}\alpha_{nmk}\cos\frac{m\pi s}{L}q_{nmk} \qquad \text{(C4a)}$$

$$v_n(s) = \sum_{m=1}^{M} \sum_{k=1}^{3} \beta_{nmk} \sin \frac{m\pi s}{L} q_{nmk} \tag{C4b}$$

$$w_n(s) = \sum_{m=1}^{M} \sum_{k=1}^{3} \gamma_{nmk} \sin \frac{m\pi s}{L} q_{nmk} \tag{C4c}$$

Here m represents the number of meridional half-waves in the mode shape and M is the largest value of m in the expansion. The inner summation with index k is used to account for the fact that corresponding to a given nodal pattern defined by n and m there are three modes. The relative amplitudes of u_n, v_n, and w_n in a given mode are given by α_{nmk}, β_{nmk}, and γ_{nmk}, respectively, and the generalized coordinate associated with a mode is denoted by q_{nmk}. The coordinates q_{nmk} are calculated by the principle of minimum potential energy. Substituting equations (C4) into the strain energy in equation (C3), integrating with respect to s, and minimizing the resulting expression with respect to each of the unknowns q_{nmk} give the following formula:

$$q_{nmk} = \frac{\frac{E\alpha hr}{1-\nu} P_{nm} \left(-\lambda_m \alpha_{nmk} + \frac{n}{r} \beta_{nmk} + \frac{\gamma_{nmk}}{r} \right)}{\bar{K}_{11} \alpha_{nmk}^2 + \bar{K}_{22} \beta_{nmk}^2 + \bar{K}_{33} \gamma_{nmk}^2 + 2\bar{K}_{12} \alpha_{nmk} \beta_{nmk} + 2\bar{K}_{13} \alpha_{nmk} \gamma_{nmk} + 2\bar{K}_{23} \beta_{nmk} \gamma_{nmk}} \tag{C5}$$

where

$$\left.\begin{aligned} \lambda_m &= \frac{m\pi}{L} \\ P_{nm} &= \int_0^L T_n(s) \sin \lambda_m s \, ds \end{aligned}\right\} \tag{C6}$$

and the stiffness coefficients are defined as follows:

$$\bar{K}_{11} = \frac{C_n L r}{2} \left(C \lambda_m^2 + C \frac{1-\mu}{2} \frac{n^2}{r^2} \right) \tag{C7a}$$

$$\bar{K}_{12} = -\frac{C_n Lr}{2}\left(\frac{C\mu n}{r}\lambda_m + \frac{C}{2}\frac{1-\mu}{r}n\lambda_m\right) \tag{C7b}$$

$$\bar{K}_{13} = -\frac{C_n Lr}{2}\frac{C\mu}{r}\lambda_m \tag{C7c}$$

$$\bar{K}_{22} = \frac{C_n Lr}{2}\left(\frac{Cn^2}{r^2} + C\frac{1-\mu}{2}\lambda_m^2 + \frac{Dn^2}{r^4} + D\frac{1-\mu}{2}\frac{\lambda_m^2}{r^2}\right) \tag{C7d}$$

$$\bar{K}_{23} = \frac{C_n Lr}{2}\left[\frac{Cn}{r^2} + \frac{Dn^3}{r^4} + \frac{D\mu n}{r^2}\lambda_m^2 + \frac{Dn(1-\mu)}{r^2}\lambda_m^2\right] \tag{C7e}$$

$$\bar{K}_{33} = \frac{C_n Lr}{2}\left[\frac{Cn}{r^2} + D\lambda_m^4 + \frac{Dn^4}{r^4} + 2\mu D\frac{n^2}{r^2}\lambda_m^2 + 2D(1-\mu)\frac{n^2}{r^2}\lambda_m^2\right] \tag{C7f}$$

where P_{mn} is the generalized force for the mode characterized by n and m. The modal amplitudes α_{nmk}, β_{nmk}, and γ_{nmk} are all that now remain to be calculated. They are computed by a modal analysis described in the next section.

Determination of α_{nmk}, β_{nmk}, and γ_{nmk}

The relative amplitudes α_{nmk}, β_{nmk}, and γ_{nmk} are obtained by a normal mode analysis based on the shapes shown in equation (C4). Making use of these equations, but noting that for free vibrations the modal coordinates q_{nmk} instead of being constant have simple-harmonic time variations, gives:

$$\left.\begin{aligned} u_n(s,t) &= \sum_{m=1}^{M}\sum_{k=1}^{3}\alpha_{nmk}\cos\lambda_m s\, e^{i\omega_{nmk}t} \\ v_n(s,t) &= \sum_{m=1}^{M}\sum_{k=1}^{3}\beta_{nmk}\sin\lambda_m s\, e^{i\omega_{nmk}t} \\ w_n(s,t) &= \sum_{m=1}^{M}\sum_{k=1}^{3}\gamma_{nmk}\sin\lambda_m s\, e^{i\omega_{nmk}t} \end{aligned}\right\} \tag{C8}$$

where ω_{nmk} is the natural frequency associated with the mode shape characterized by the triplet n,m,k. The strain energy U and the kinetic energy T^* are written as

$$U = \frac{1}{2} \{\bar{\alpha}\}^T [\bar{K}] \{\bar{\alpha}\} e^{2\omega_{nmk} t} \tag{C9}$$

$$T^* = \frac{1}{2} \omega_{nmk}^2 \{\bar{\alpha}\}^T [\bar{M}] \{\bar{\alpha}\} e^{2\omega_{nmk} t} \tag{C10}$$

where

$$\{\bar{\alpha}\} = \begin{Bmatrix} \alpha_{nmk} \\ \beta_{nmk} \\ \gamma_{nmk} \end{Bmatrix}$$

and

$$[\bar{M}] = \frac{\pi r L \rho h}{2} [I]$$

with [I] being a 3×3 identity matrix. Applying the principle of minimum potential energy along with equations (C9) and (C10) gives the following modal equation:

$$[\bar{K}] \{\bar{\alpha}\} = \omega_{nmk}^2 [\bar{M}] \{\bar{\alpha}\}$$

This eigenvalue problem is solved by use of the threshold Jacobi method described in reference 9.

Effect of Length on Thermal Stresses in a Cylinder With a Heated Generator

In reference 3 a solution is obtained for the axial stress resultant in a cylinder of infinite length and used for predicting such a stress in finite cylinders. It was of interest in connection with the present work to assess the range of cylinder geometry for which the infinite cylinder solution is applicable to finite cylinders. Thus, a number of calculations using the exact modal method of appendix B were carried out in which all the shell dimensions were fixed except the length-to-radius ratio which was varied from 1 to 1000. The results are shown in figure 10.

APPENDIX C

The infinite cylinder solution is denoted by the broken line. It is of course constant. For $L/r = 1$, the axial stress is 0. For $L/r = 10$, the curve attains a compressive stress at the center of the cylinder which exceeds the infinite cylinder stress by about 9 percent. For $L/r = 100$ and 1000, the stress is constant and equal to the infinite cylinder solution outside a narrow boundary layer adjacent to each edge. At the beginning of boundary layer, a value of stress is reached which exceeds the infinite-cylinder solution by about 4 percent. The conclusion from this study is that the infinite-cylinder solution is a good approximation for the stresses in the interior of a long cylinder (L/r greater than or equal to about 100) but underestimates the stress near the edges. The infinite cylinder solution is furthermore found to be completely erroneous for cylinders having L/r less than 10.

REFERENCES

1. Boresi, A. P.: General Investigation of Thin Shells Including the Effect of Nonhomogeneous Temperature Distribution. TAM Rep. No. 177 (Contract No. NR 1834(14)), Univ. of Illinois, Aug. 1960.

2. Eisentraut, R. A.: Thermal Stresses in Cylindrical Shells. Tech. Rep. No. 112 (Contract Nonr 225(16)), Div. Eng. Mech., Stanford Univ., Oct. 30, 1957.

3. Ong, Chung-Chun: Effects of Thermal Stresses on Free Vibrations of Thin Cylindrical Shells. Ph. D. Diss., Northwestern Univ., Aug. 1967.

4. Bushnell, David; and Smith, Strether: Stress and Buckling of Nonuniformly Heated Cylindrical and Conical Shells. AIAA J., vol. 9, no. 12, Dec. 1971, pp. 2314-2321.

5. Anderson, M. S.; Fulton, R. E.; Heard, W. L., Jr.; and Walz, J. E.: Stress, Buckling, and Vibration Analysis of Shells of Revolution. Computers & Structures, vol. 1, nos. 1/2, Aug. 1971, pp. 157-192.

6. Stephens, Wendell B.: Computer Program for Static and Dynamic Axisymmetric Nonlinear Response of Symmetrically Loaded Orthotropic Shells of Revolution. NASA TN D-6158, 1970.

7. Cohen, Gerald A.: Computer Analysis of Asymmetrical Deformation of Orthotropic Shells of Revolution. AIAA J., vol. 2, no. 5, May 1964, pp. 932-934.

8. MacNeal, Richard H., ed.: The NASTRAN Theoretical Manual (Level 15). NASA SP-221(01), 1972.

9. Adelman, Howard M.; Catherines, Donnell S.; and Walton, William C., Jr.: A Method for Computation of Vibration Modes and Frequencies of Orthotropic Thin Shells of Revolution Having General Meridional Curvature. NASA TN D-4972, 1969.

10. Adelman, Howard M.; Catherines, Donnell S.; Steeves, Earl C.; and Walton, William C., Jr.: User's Manual for a Digital Computer Program for Computing the Vibration Characteristics of Ring-Stiffened Orthotropic Shells of Revolution. NASA TM X-2138, 1970.

11. Adelman, Howard M.; and Catherines, Donnell S.: Calculation of Temperature Distributions in Thin Shells of Revolution by the Finite-Element Method. NASA TN D-6100, 1971.

12. Adelman, Howard M.; Catherines, Donnell S.; and Walton, William C., Jr.: Accuracy of Modal Stress Calculations by the Finite Element Method. AIAA J., vol. 8, no. 3, Mar. 1970, pp. 462-468.

13. Boley, Bruno A.; and Weiner, Jerome H.: Theory of Thermal Stresses. John Wiley & Sons, Inc., c.1960, p. 263.

14. Huth, J. H.: Thermal Stresses in Conical Shells. J. Aeronaut. Sci., vol. 20, no. 9, Sept. 1953, pp. 613-616.

15. Kraus, Harry: Thin Elastic Shells. John Wiley & Sons, Inc., c.1967.

TABLE 1.- STIFFNESSES OF AN ORTHOTROPIC SHELL AS USED IN EQUATION (5)

[Subscripts 1 and 2 refer to meridional and circumferential directions, respectively]

$$C_{11} = \int_z \frac{E_1}{1 - \mu_1\mu_2}\, dz \qquad C_{12} = \int_z \frac{\mu_1 E_2}{1 - \mu_1\mu_2}\, dz$$

$$C_{22} = \int_z \frac{E_2}{1 - \mu_1\mu_2}\, dz \qquad C_{66} = \int_z G\, dz$$

$$D_{11} = \int_z \frac{E_1}{1 - \mu_1\mu_2}\, z^2\, dz \qquad D_{12} = \int_z \frac{\mu_1 E_2}{1 - \mu_1\mu_2}\, z^2\, dz$$

$$D_{22} = \int_z \frac{E_2}{1 - \mu_1\mu_2}\, z^2\, dz \qquad D_{66} = 4 \int_z Gz^2\, dz$$

$$K_{11} = \int_z \frac{E_1}{1 - \mu_1\mu_2}\, z\, dz \qquad K_{12} = 2 \int \frac{\mu_1 E_2}{1 - \mu_1\mu_2}\, z\, dz$$

$$K_{22} = \int_z \frac{E_2}{1 - \mu_1\mu_2}\, z\, dz \qquad K_{66} = \int Gz\, dz$$

TABLE 2.- EDGE CONSTRAINTS

Description	Equations for edge constraint	Rows and columns deleted
Free-free	None	None
Free—freely supported	$v(L) = w(L) = 0$	$7K+1, 7K+3$
Freely supported—free	$v(0) = w(0) = 0$	1,3
Free—simply supported	$u(L) = v(L) = w(L) = 0$	$7K+1, 7K+2, 7K+3$
Simply supported—free	$u(0) = v(0) = \omega(0) = 0$	1,2,3
Free-clamped	$u(L) = v(L) = w(L) = \beta(L) = 0$	$7K+1, 7K+2, 7K+3, 7K+4$
Clamped-free	$u(0) = v(0) = w(0) = \beta(0) = 0$	1,2,3,4
Freely supported—freely supported	$v(0) = w(0) = 0$ $v(L) = w(L) = 0$	$1,3, 7K+1, 7K+3$
Simply supported—simply supported	$u(0) = v(0) = w(0) = 0$ $u(L) = v(L) = w(L) = 0$	$1,2,3, 7K+1, 7K+2, 7K+3$
Clamped—clamped	$u(0) = v(0) = w(0) = \beta(0) = 0$	$1,2,3,4, 7K+1, 7K+2, 7K+3, 7K+4$
Freely supported—simply supported	$v(0) = w(0) = 0$ $u(L) = v(L) = w(L) = 0$	$1,3, 7K+1, 7K+2, 7K+3$
Freely supported—clamped	$v(0) = w(0) = 0$ $u(L) = v(L) = w(L) = \beta(L) = 0$	$1,3, 7K+1, 7K+2, 7K+3, 7K+4$
Simply supported—freely supported	$u(0) = v(0) = w(0) = 0$ $v(L) = w(L) = 0$	$1,2,3, 7K+1, 7K+3$
Simply supported—clamped	$u(0) = v(0) = w(0) = 0$ $u(L) = v(L) = w(L) = \beta(L) = 0$	$1,2,3, 7K+1, 7K+2, 7K+3, 7K+4$
Clamped—freely supported	$u(0) = v(0) = w(0) = \beta(0) = 0$ $v(L) = w(L) = 0$	$1,2,3,4, 7K+1, 7K+3$
Clamped—simply supported	$u(0) = v(0) = w(0) = \beta(0) = 0$ $u(L) = v(L) = w(L) = 0$	$1,2,3,4, 7K+1, 7K+2, 7K+3$

TABLE 3.- FINITE-ELEMENT REPRESENTATIONS OF SHELLS USED FOR SAMPLE CALCULATIONS

Nondimensional element length, ϵ_k/L, for –				
Cylinder I 14 elements	Cylinder II 10 elements	Conical frustum 19 elements	Hemisphere 14 elements	Annular plate 10 elements
0.025	0.1	0.00833	0.02	0.1
.025	.1	.00833	.02	.1
.025	.1	.00833	.05	.1
.025	.1	.00833	.05	.1
.050	.1	.0166	.12	.1
.050	.1	.0166	.12	.1
.300	.1	.0166	.12	.1
.300	.1	.1666	.12	.1
.050	.1	.1666	.12	.1
.050	.1	.1666	.12	.1
.025		.1666	.05	
.025		.1666	.05	
.025		.0166	.02	
.025		.0166	.02	
		.0166		
		.00833		
		.00833		
		.00833		
		.00833		

TABLE 4.- STRESS RESULTANTS FOR A CLAMPED-CLAMPED CYLINDER WITH A HEATED MIDLENGTH

s/L	$T_1/Eh\alpha T$		$T_2/Eh\alpha t$	
	Present solution	Analytical solution (ref. 3)	Present solution	Analytical solution (ref. 3)
0	-0.548395	-0.548412	-0.137099	-0.137103
.1	-.548250	-.548412	-.235410	-.235451
.2	-.545230	-.548412	-.224090	-.224887
.3	-.549768	-.548412	-.204163	-.203382
.4	-.546987	-.548412	-.244610	-.243848
.5	-.551681	-.548412	-.396033	-.395210
.6	-.546987	-.548412	-.244610	-.243848
.7	-.549768	-.548412	-.204163	-.203382
.8	-.545230	-.548412	-.224090	-.224887
.9	-.548250	-.548412	-.235410	-.235451
1.0	-.548395	-.548412	-.137099	-.137103

TABLE 5.- CIRCUMFERENTIAL STRESS RESULTANTS FOR A FREELY SUPPORTED CYLINDER WITH A HEATED GENERATOR

s/L	$T_2/Eh\alpha T$ for –				
	n = 0 (a)	n = 1 (a)	n = 2 (a)	n = 3 (a)	n = 4 (a)
0	-0.316899 -.311717	-0.316912 -.311717	-0.126781 -.124687	-0.063403 -.062344	-0.037307 -.036674
0.1	-0.024860 -.024696	-0.025348 -.025184	-0.010746 -.010682	-0.005923 -.005891	-0.004000 -.003982
0.2	0.020494 .020413	0.030190 .020108	0.007665 .007630	0.003399 .003381	0.001511 .001499
0.3	0.005148 .005102	0.005147 .005099	0.002004 .001982	0.000846 .000833	0.000203 .000194
0.4	-0.000788 -.000792	-0.000752 -.000758	-0.000308 -.000313	-0.000267 -.000272	-0.000422 -.000426
0.5	-0.001020 -.001015	-0.001007 -.001004	-0.000435 -.000437	-0.000349 -.000352	-0.000484 -.000488
0.6	-0.000788 -.000792	-0.000752 -.000758	-0.000308 -.000313	-0.000267 -.000272	-0.000422 -.000426
0.7	0.005148 .005102	0.005147 .005099	0.002004 .001982	0.000846 .000833	0.000203 .000194
0.8	0.020494 .020413	0.020190 .020108	0.007665 .007630	0.003399 .003381	0.001511 .001499
0.9	-0.024860 -.024696	-0.025348 -.025184	-0.010746 -.010682	-0.005923 -.005891	-0.004000 -.003982
1.0	-0.316899 -.311717	-0.316912 -.311717	-0.126781 -.124687	-0.063403 -.062344	-0.037307 -.036674

[a] Top line – present solution
Bottom line – analytical solution (appendix C)

TABLE 6.- MERIDIONAL STRESS RESULTANT FOR A CLAMPED ORTHOTROPIC CONE

s/L	$T_1/E_1 h \alpha_1 T_{max}$		
	Present solution	SADAOS (ref. 6)	SALORS (ref. 5)
0	67.9152	68.5935	71.52
.1	34.8894	34.9249	34.90
.2	23.1281	23.2835	23.26
.3	17.5112	17.4625	17.45
.4	13.9475	13.9699	13.96
.5	11.6352	11.6416	11.63
.6	9.98591	9.97855	9.969
.7	8.72492	8.73126	8.727
.8	7.76298	7.76115	7.757
.9	6.98650	6.98525	6.981
1.0	6.49627	6.49742	6.680

TABLE 7.- STRESS RESULTANTS IN A CLAMPED TRUNCATED HEMISPHERE

s/L	$T_1/Eh\alpha T_{max}$		$T_2/Eh\alpha T_{max}$	
	Present solution	SALORS (ref. 5)	Present solution	SALORS (ref. 5)
0	-0.04843	-0.05115	-0.5145	-0.5155
.1	-.05076	-.04968	-.1583	-.1571
.2	-.05077	-.05065	.06259	.06220
.3	-.05339	-.05445	.07233	.07230
.4	-.05813	-.05895	.06007	.06046
.5	-.06430	-.06485	.06168	.06225
.6	-.07224	-.07325	.07493	.07550
.7	-.08469	-.08630	.11291	.1129
.8	-.10697	-.1065	.12873	.1272
.9	-.12065	-.1185	-.22234	-.2239
1.0	-.03444	-.03821	-1.0103	-1.012

TABLE 8.- MOMENT RESULTANTS FOR A CLAMPED ANNULAR PLATE

s/L	$M_1/Eh^3\alpha T_{max}$		$M_2/Eh^3\alpha T_{max}$	
	Present solution	Analytical solution (appendix C)	Present solution	Analytical solution (appendix C)
0	1.80057	1.80055	2.62350	2.62350
.1	3.11838	3.16188	3.39046	3.53529
.2	4.28310	4.33328	4.20909	4.37560
.3	5.33251	5.37015	5.06365	5.18880
.4	6.29431	6.31184	5.94524	6.00328
.5	7.18740	7.18419	6.84879	6.83769
.6	8.02591	8.00600	7.77156	7.70467
.7	8.82060	8.79099	8.71221	8.61293
.8	9.57974	9.54944	9.67016	9.56858
.9	10.3098	10.2892	10.6454	10.5760
1.0	11.0161	11.0163	11.6381	11.6382

TABLE 9.- ELEMENTS OF MATRIX $[T_k]$

$$
\begin{bmatrix}
\frac{1}{2} & \frac{\epsilon_k}{32R_{1,k}}\left(5-\frac{\epsilon_k R'_{1,k}}{2R_{1,k}}\right) & 0 & \frac{5\epsilon_k}{32} & \frac{\epsilon_k^2}{64R_{1,k}} & 0 & \frac{\epsilon_k^2}{64} & \frac{1}{2} & -\frac{\epsilon_k}{32R_{1,k+1}}\left(5+\frac{\epsilon_k R'_{1,k+1}}{2R_{1,k+1}}\right) & 0 & -\frac{5\epsilon_k}{32} & \frac{\epsilon_k^2}{64R_{1,k+1}} & 0 & \frac{\epsilon_k^2}{64} \\
-\frac{15}{8\epsilon_k} & \frac{1}{16R_{1,k}}\left(-7+\frac{\epsilon_k R'_{1,k}}{2R_{1,k}}\right) & 0 & -\frac{7}{16} & -\frac{\epsilon_k}{32R_{1,k}} & 0 & -\frac{\epsilon_k}{32} & \frac{15}{8\epsilon_k} & -\frac{1}{16R_{1,k+1}}\left(7+\frac{\epsilon_k R'_{1,k+1}}{2R_{1,k+1}}\right) & 0 & -\frac{7}{16} & \frac{\epsilon_k}{32R_{1,k+1}} & 0 & \frac{\epsilon_k}{32} \\
0 & \frac{1}{4\epsilon_k R_{1,k}}\left(-3+\frac{\epsilon_k R'_{1,k}}{2R_{1,k}}\right) & 0 & -\frac{3}{4\epsilon_k} & -\frac{1}{8R_{1,k}} & 0 & -\frac{1}{8} & 0 & \frac{1}{4\epsilon_k R_{1,k+1}}\left(3+\frac{\epsilon_k R'_{1,k+1}}{2R_{1,k+1}}\right) & 0 & \frac{3}{4\epsilon_k} & -\frac{1}{8R_{1,k+1}} & 0 & -\frac{1}{8} \\
\frac{5}{\epsilon_k^3} & \frac{1}{2\epsilon_k^2 R_{1,k}}\left(5-\frac{\epsilon_k R'_{1,k}}{2R_{1,k}}\right) & 0 & \frac{5}{2\epsilon_k^2} & \frac{1}{4\epsilon_k R_{1,k}} & 0 & \frac{1}{4\epsilon_k} & -\frac{5}{\epsilon_k^3} & \frac{1}{2\epsilon_k^2 R_{1,k+1}}\left(5+\frac{\epsilon_k R'_{1,k+1}}{2R_{1,k+1}}\right) & 0 & \frac{5}{2\epsilon_k^2} & -\frac{1}{4\epsilon_k R_{1,k+1}} & 0 & -\frac{1}{4\epsilon_k} \\
0 & \frac{1}{2\epsilon_k^3 R_{1,k}}\left(1-\frac{\epsilon_k R'_{1,k}}{2R_{1,k}}\right) & 0 & \frac{1}{2\epsilon_k^3} & \frac{1}{4\epsilon_k^2 R_{1,k}} & 0 & \frac{1}{4\epsilon_k^2} & 0 & -\frac{1}{2\epsilon_k^3 R_{1,k+1}}\left(1+\frac{\epsilon_k R'_{1,k+1}}{2R_{1,k+1}}\right) & 0 & -\frac{1}{2\epsilon_k^3} & \frac{1}{4\epsilon_k^2 R_{1,k+1}} & 0 & \frac{1}{4\epsilon_k^2} \\
-\frac{6}{\epsilon_k^5} & \frac{1}{\epsilon_k^4 R_{1,k}}\left(-3+\frac{\epsilon_k R'_{1,k}}{2R_{1,k}}\right) & 0 & -\frac{3}{\epsilon_k^4} & -\frac{1}{2\epsilon_k^3 R_{1,k}} & 0 & -\frac{1}{2\epsilon_k^3} & \frac{6}{\epsilon_k^5} & -\frac{1}{\epsilon_k^4 R_{1,k+1}}\left(3+\frac{\epsilon_k R'_{1,k+1}}{2R_{1,k+1}}\right) & 0 & -\frac{3}{\epsilon_k^4} & \frac{1}{2\epsilon_k^3 R_{1,k+1}} & 0 & \frac{1}{2\epsilon_k^3} \\
0 & \frac{1}{2} & 0 & 0 & \frac{\epsilon_k}{8} & 0 & 0 & 0 & \frac{1}{2} & 0 & 0 & -\frac{\epsilon_k}{8} & 0 & 0 \\
0 & -\frac{3}{2\epsilon_k} & 0 & 0 & -\frac{1}{4} & 0 & 0 & 0 & \frac{3}{2\epsilon_k} & 0 & 0 & -\frac{1}{4} & 0 & 0 \\
0 & 0 & 0 & 0 & -\frac{1}{2\epsilon_k} & 0 & 0 & 0 & 0 & 0 & 0 & \frac{1}{2\epsilon_k} & 0 & 0 \\
0 & \frac{2}{\epsilon_k^3} & 0 & 0 & \frac{1}{\epsilon_k^2} & 0 & 0 & 0 & -\frac{2}{\epsilon_k^3} & 0 & 0 & \frac{1}{\epsilon_k^2} & 0 & 0 \\
0 & 0 & \frac{1}{2} & 0 & 0 & \frac{\epsilon_k}{8} & 0 & 0 & 0 & \frac{1}{2} & 0 & 0 & -\frac{\epsilon_k}{8} & 0 \\
0 & 0 & -\frac{3}{2\epsilon_k} & 0 & 0 & -\frac{1}{4} & 0 & 0 & 0 & \frac{3}{2\epsilon_k} & 0 & 0 & -\frac{1}{4} & 0 \\
0 & 0 & 0 & 0 & 0 & -\frac{1}{2\epsilon_k} & 0 & 0 & 0 & 0 & 0 & 0 & \frac{1}{2\epsilon_k} & 0 \\
0 & 0 & \frac{2}{\epsilon_k^3} & 0 & 0 & \frac{1}{\epsilon_k^2} & 0 & 0 & 0 & -\frac{2}{\epsilon_k^3} & 0 & 0 & \frac{1}{\epsilon_k^2} & 0
\end{bmatrix}
$$

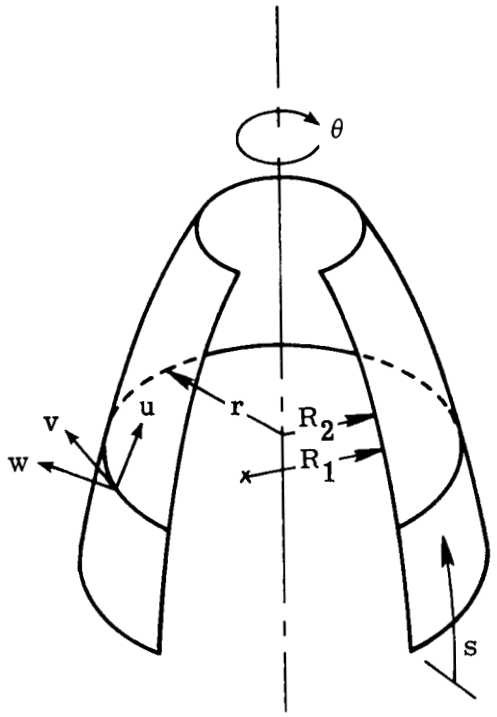

(a) Coordinate system and displacement component directions.

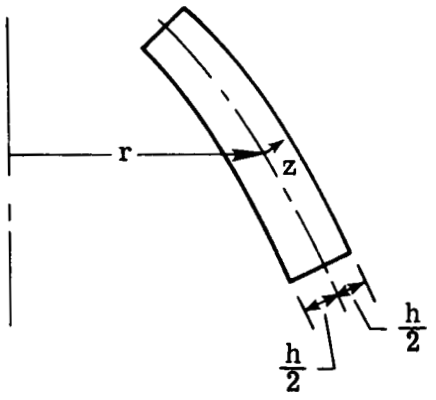

(b) Detail of shell wall.

Figure 1.- Geometry of a shell of revolution.

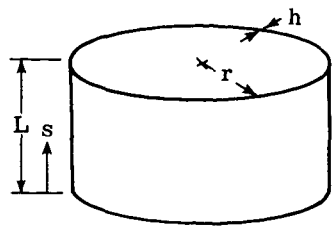

$E = 10$ GPa $\quad r = 1.0$ m

$\alpha = 1 \times 10^{-5}$/K $\quad L = 1.0$ m

$h = 10$ cm $\quad \mu = 0.25$

$$T_o = T_i = \begin{cases} \dfrac{\sinh (s/L)}{\sinh (1/2)} & (0 \leq s/L \leq 1/2) \\ \dfrac{\sinh (1-s/L)}{\sinh (1/2)} & (1/2 \leq s/L \leq 1) \end{cases}$$

(a) Cylinder with heated midlength – clamped edges (cylinder I).

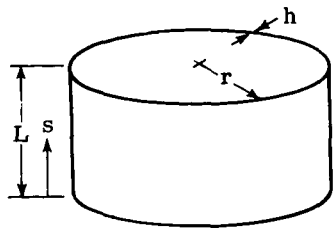

$h = 1$ cm $\quad L = 1.0$ m $\quad \alpha = 1 \times 10^{-6}$/K

$r = 1.0$ m $\quad E = 10$ GPa $\quad \mu = 0.3$

$$T_o = T_i = \sum_n T \cos n\theta$$

$$T = \begin{cases} \dfrac{1}{\pi} \tanh \pi & (n = 0) \\ \dfrac{2}{\pi (1 + n^2)} \tanh \pi & (n > 0) \end{cases}$$

(b) Cylinder with heated generator – freely supported edges (cylinder II).

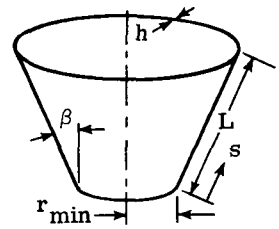

$h = 0.0625$ cm $\quad T_o = 1500 - 1000\,(s/L) + 500\,(s/L)^2$

$\beta = 30^o$ $\quad T_i = 500$

$L = 120$ cm $\quad \mu_1 = 0.25$

$r_{min} = 60$ cm $\quad \mu_2 = 0.20$

$E_1 = 50$ GPa $\quad \alpha_1 = 6.67 \times 10^{-6}$/K

$E_2 = 40$ GPa $\quad \alpha_2 = 6.08 \times 10^{-6}$/K

(c) Conical frustum – clamped edges.

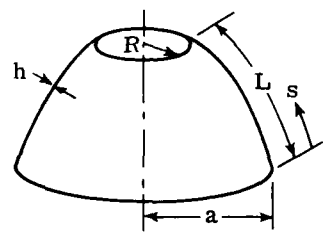

$h = 1$ cm $\quad \alpha = 1 \times 10^{-6}$/K

$L = 1.0$ m $\quad \mu = 0.3$

$a = 1.0$ m $\quad R = 0.540$ m

$E = 10$ GPa

$$T_o = T_i = 1 + 0.6587 \log \left[\frac{1 + \sin (s/L)}{1 - \sin (s/L)} \right] + \cos (s/L)$$

(d) Truncated hemisphere – clamped edges.

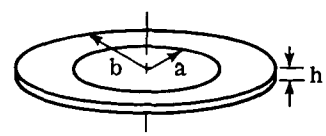

$a = 1.0$ m $\quad \alpha = 1 \times 10^{-3}$/K

$b = 2.0$ m $\quad L = r_2 - r_1$

$h = 1$ cm $\quad \mu = 0.3$

$E = 100$ GPa $\quad T_o - T_i = 2000\,(1 + s/L)^2$

(e) Annular plate – clamped edges.

Figure 2.- Models used for sample calculations.
All temperatures are in K.

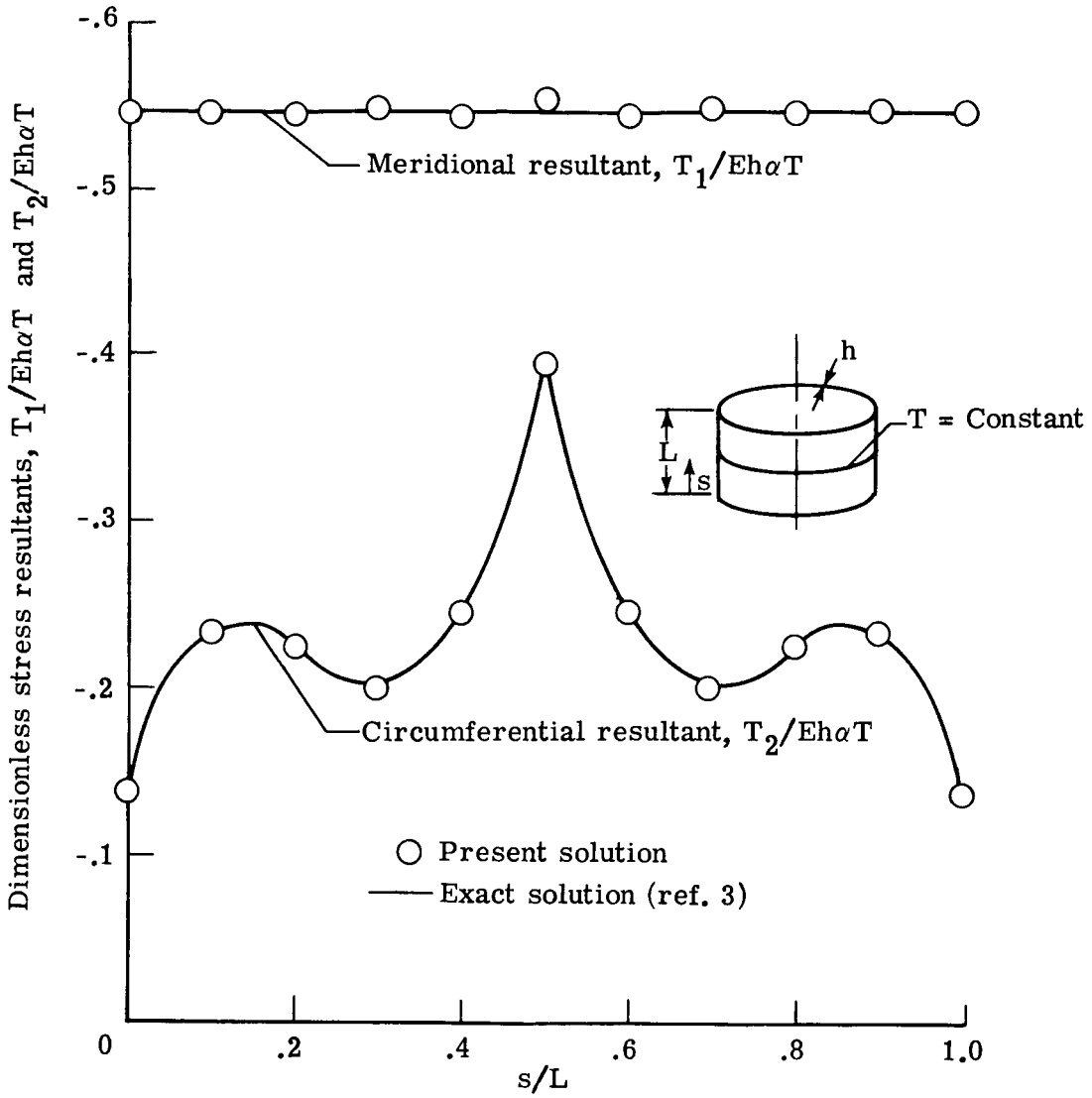

Figure 3.- Stress resultants in cylinder with prescribed midlength temperature. Both edges clamped; cylinder I.

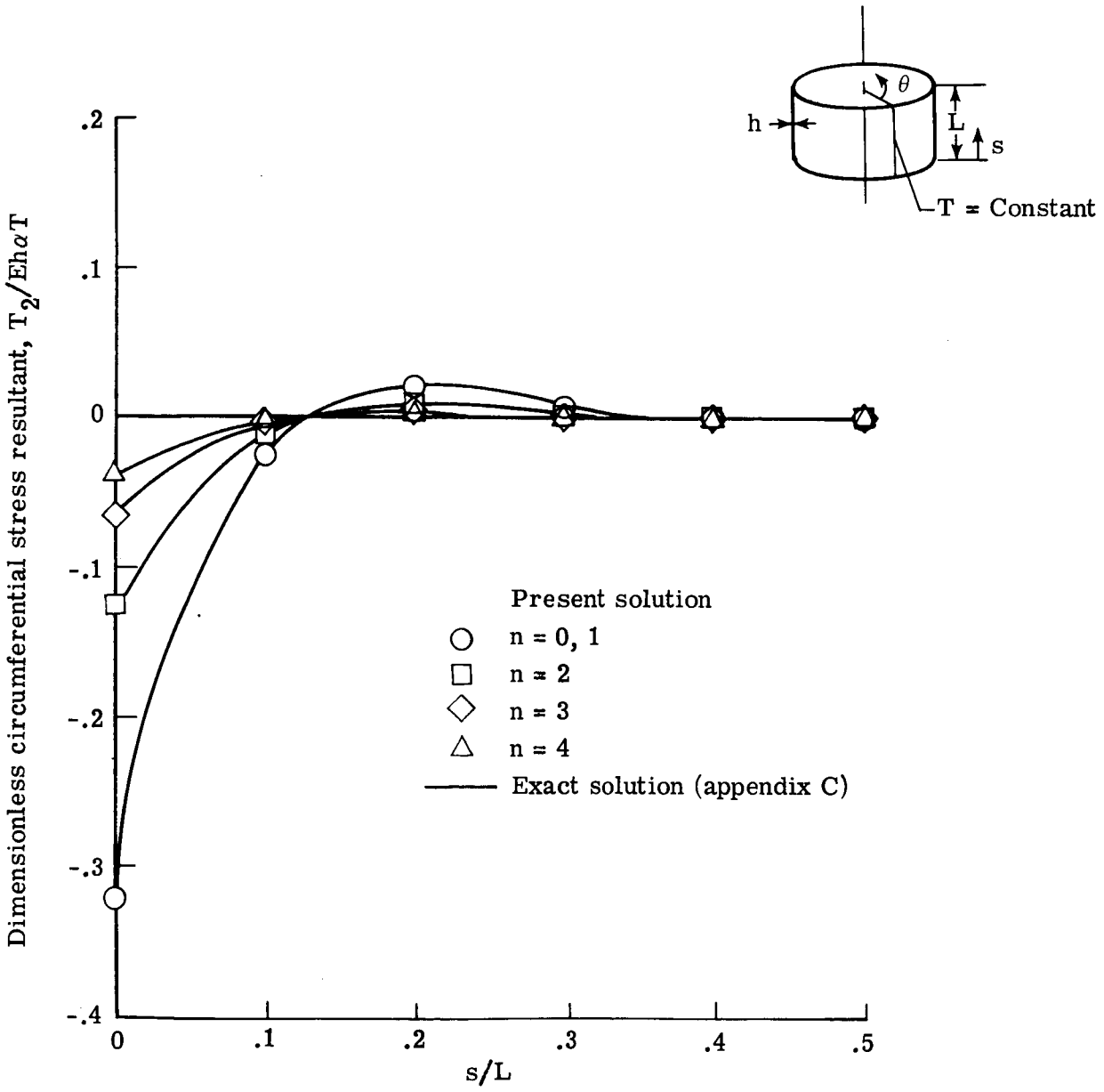

Figure 4.- Circumferential stress resultant in cylinder with heated generator. Both edges clamped.

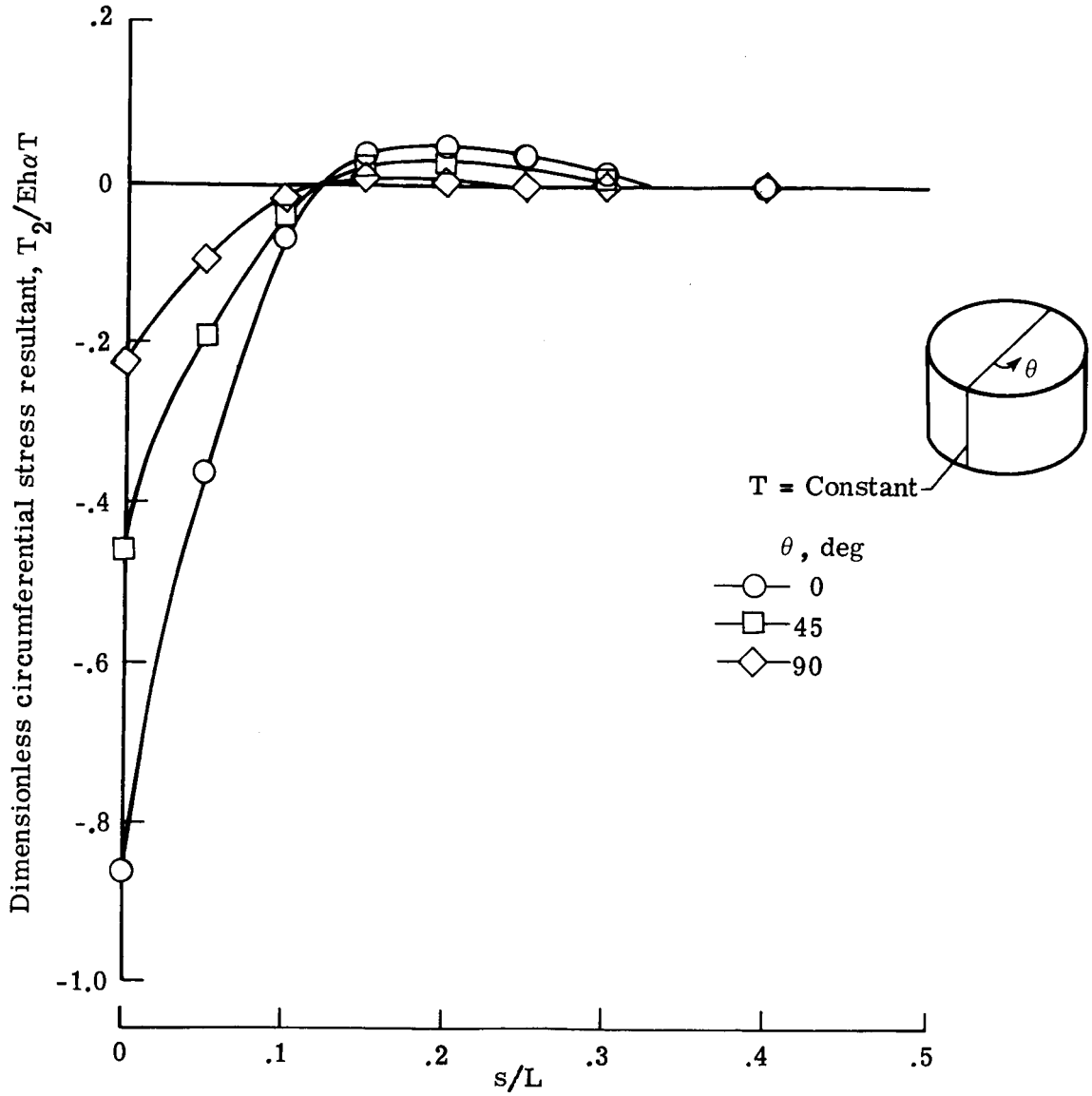

Figure 5.- Circumferential stress resultant as a function of circumferential angle for cylinder heated along a generator. Both edges freely supported; present method.

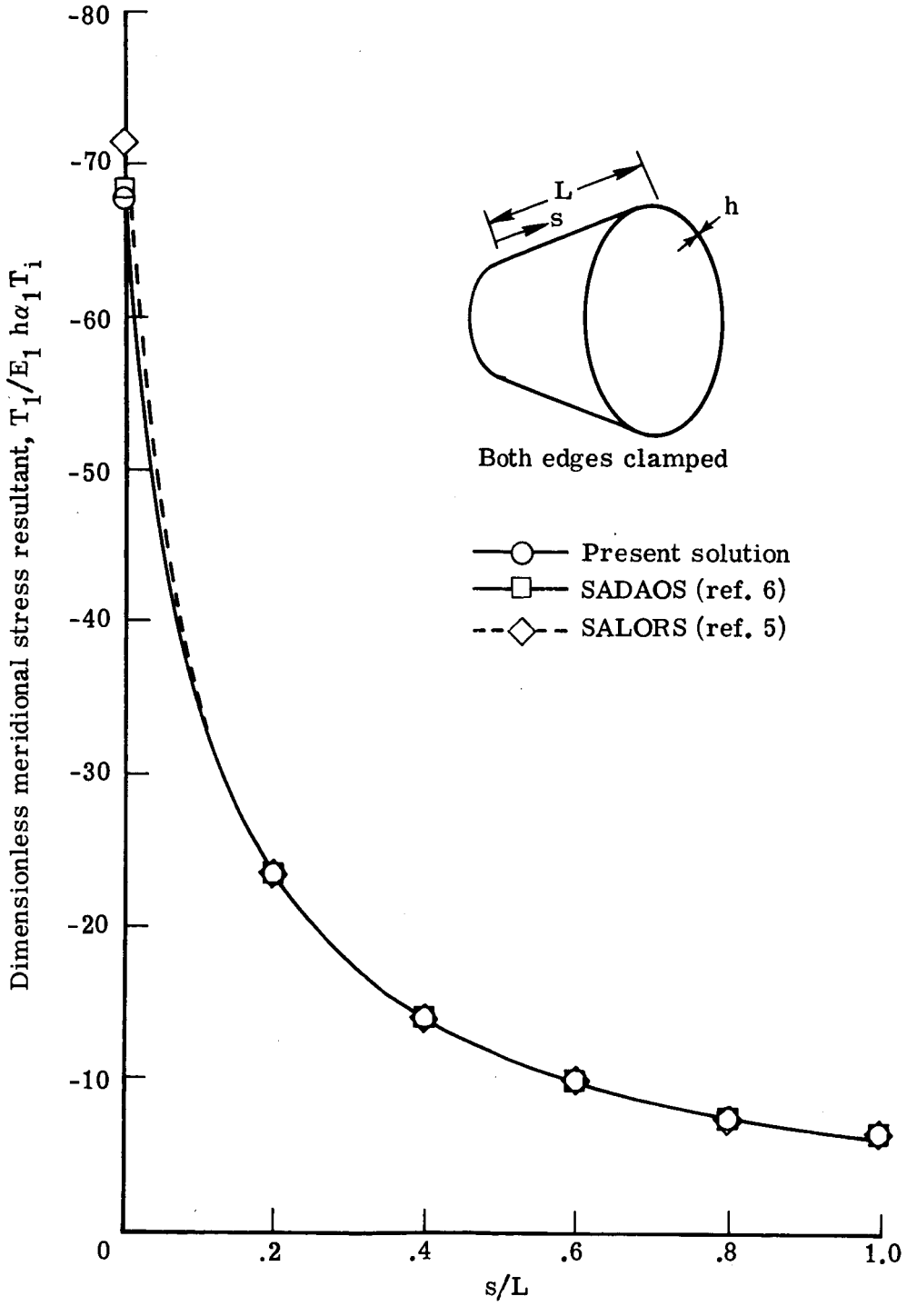

Figure 6.- Meridional stress resultant in orthotropic 30° conical frustum. Both edges clamped; $T_o = 1500 - 1000(s/L) + 500(s/L)^2$; $T_i = 500$.

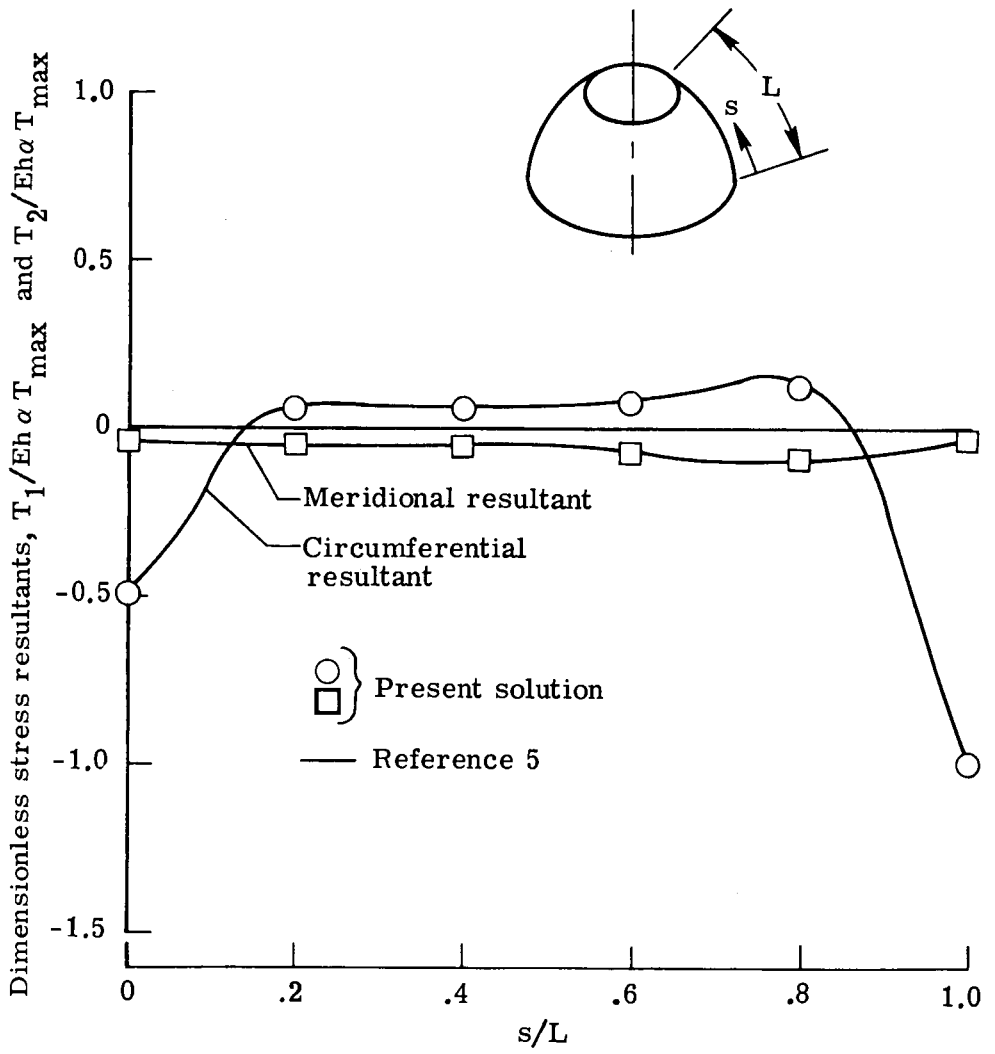

Figure 7.- Stress resultants in truncated hemisphere. Both edges clamped;

$$T_o = T_i = 1 + 0.6587 \log\left[\frac{1 + \sin(s/L)}{1 - \sin(s/L)}\right] + \cos(s/L).$$

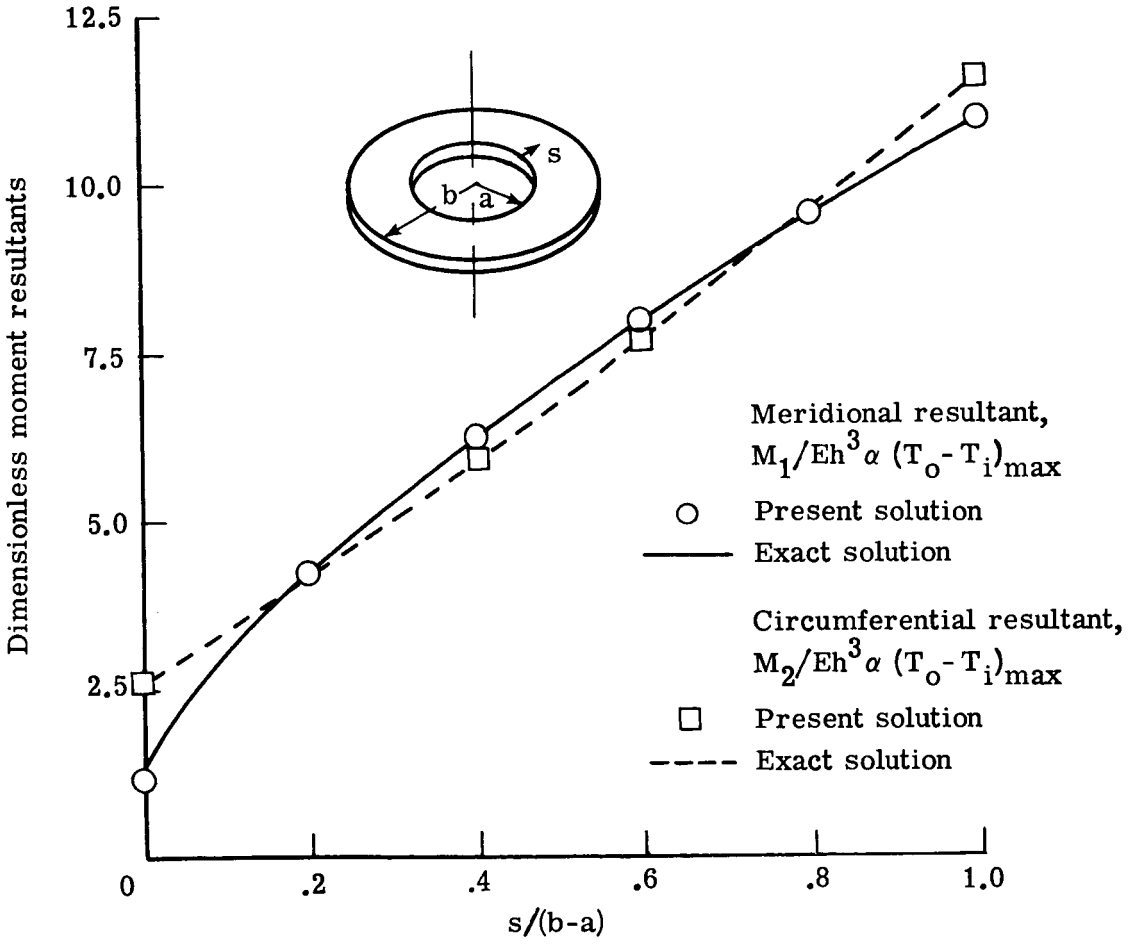

Figure 8.- Moment resultants in annular plate. Both edges clamped;

$$T_o = T_i = 2000\left(1 + \frac{s}{L}\right)^2.$$

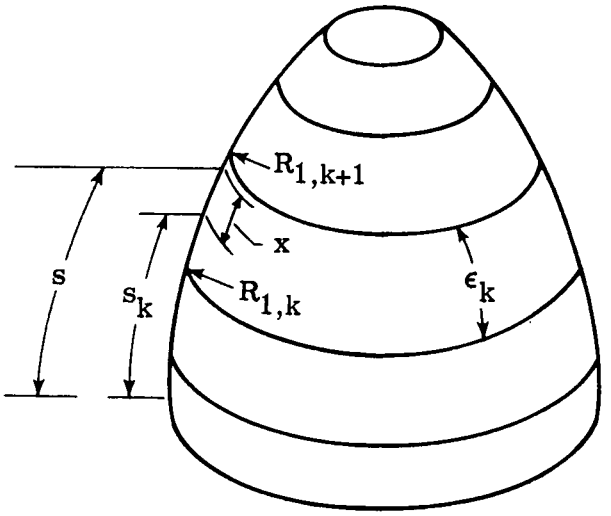

Figure 9.- Typical idealization of shell of revolution showing geometrically exact finite elements.

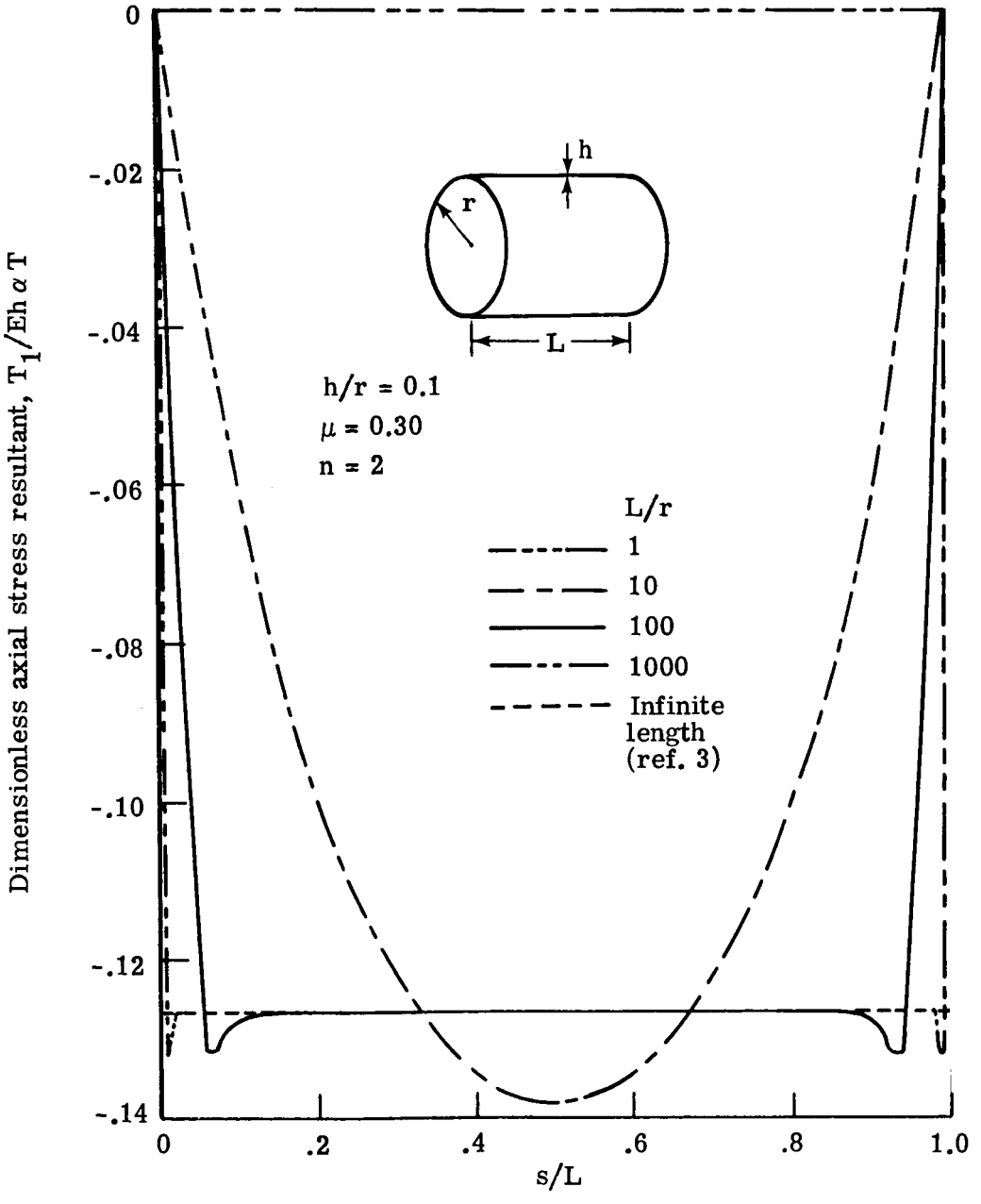

Figure 10.- Effect of length on dimensionless axial stress resultant for freely supported cylinder with heated generator.